Click here to return to USGS publications

USGS
science for a changing world

Techniques of Water-Resources Investigations
of the United States Geological Survey

Chapter D2

APPLICATION OF SEISMIC-REFRACTION TECHNIQUES TO HYDROLOGIC STUDIES

By F.P. Haeni

Book 2

COLLECTION OF ENVIRONMENTAL DATA

DEPARTMENT OF THE INTERIOR

DONALD PAUL HODEL, *Secretary*

U.S. GEOLOGICAL SURVEY

Dallas L. Peck, *Director*

UNITED STATES GOVERNMENT PRINTING OFFICE, WASHINGTON : 1988

For sale by the Books and Open-File Reports Section, U.S. Geological Survey,
Federal Center, Box 25425, Denver, CO 80225

PREFACE

The series of manuals on techniques describes procedures for planning and executing specialized work in water-resources investigations. The material is grouped under major subject headings called Books and is further subdivided into Sections and Chapters. Section D of Book 2 is on surface geophysical methods.

The unit of publication, the Chapter, is limited to a narrow field of subject matter. This format permits flexibility in revision and publication as the need arises. "Application of Seismic-Refraction Techniques to Hydrologic Studies" is Chapter D2 of Book 2.

Reference to trade names, commercial products, manufacturers, or distributors in this manual does not constitute endorsement by the U.S. Geological Survey or recommendation for use.

This manual is intended to supplement the more general "Application of Surface Geophysics to Ground-Water Investigations," by A.A.R. Zohdy, G.P. Eaton, and D.R. Mabey (U.S. Geological Survey Techniques of Water-Resources Investigations, Book 2, Chapter D1, 1974).

TECHNIQUES OF WATER-RESOURCES INVESTIGATIONS OF THE UNITED STATES GEOLOGICAL SURVEY

The U.S. Geological Survey publishes a series of manuals describing procedures for planning and conducting specialized work in water-resources investigations. The manuals published to date are listed below and may be ordered by mail from the **U.S. Geological Survey, Books and Open-File Reports, Federal Center, Box 25425, Denver, Colorado 80225** (an authorized agent of the Superintendent of Documents, Government Printing Office).

Prepayment is required. Remittance should be sent by check or money order payable to U.S. Geological Survey. Prices are not included in the listing below as they are subject to change. **Current prices can be obtained** by writing to the USGS, Books and Open File Reports. Prices include cost of domestic surface transportation. For transmittal outside the U.S.A. (except to Canada and Mexico) a surcharge of 25 percent of the net bill should be included to cover surface transportation. When ordering any of these publications, please give the title, book number, chapter number, and "U.S. Geological Survey Techniques of Water-Resources Investigations."

TWI 1-D1. Water temperature—influential factors, field measurement, and data presentation, by H.H. Stevens, Jr., J.F. Ficke, and G.F. Smoot, 1975, 65 pages.
TWI 1-D2. Guidelines for collection and field analysis of ground-water samples for selected unstable constituents, by W.W. Wood. 1976. 24 pages.
TWI 2-D1. Application of surface geophysics to ground water investigations, by A.A.R. Zohdy, G.P. Eaton, and D.R. Mabey. 1974. 116 pages.
TWI 2-E1. Application of borehole geophysics to water-resources investigations, by W.S. Keys and L.M. MacCary. 1971. 126 pages.
TWI 3-A1. General field and office procedures for indirect discharge measurement, by M.A. Benson and Tate Dalrymple. 1967. 30 pages.
TWI 3-A2. Measurement of peak discharge by the slope-area method, by Tate Dalrymple and M.A. Benson. 1967. 12 pages.
TWI 3-A3. Measurement of peak discharge at culverts by indirect methods, by G.L. Bodhaine. 1968. 60 pages.
TWI 3-A4. Measurement of peak discharge at width contractions by indirect methods, by H.F. Matthai. 1967. 44 pages.
TWI 3-A5. Measurement of peak discharge at dams by indirect methods, by Harry Hulsing. 1967. 29 pages.
TWI 3-A6. General procedure for gaging streams, by R.W. Carter and Jacob Davidian. 1968. 13 pages.
TWI 3-A7. Stage measurements at gaging stations, by T.J. Buchanan and W.P. Somers. 1968. 28 pages.
TWI 3-A8. Discharge measurements at gaging stations, by T.J. Buchanan and W.P. Somers. 1969. 65 pages.
TWI 3-A9. Measurement of time of travel and dispersion in streams by dye tracing, by E.F. Hubbard, F.A. Kilpatrick, L.A. Martens, and J.F. Wilson, Jr. 1982. 44 pages.
TWI 3-A10. Discharge ratings at gaging stations, by E.J. Kennedy. 1984. 59 pages.
TWI 3-A11. Measurement of discharge by moving-boat method, by G.F. Smoot and C.C. Novak. 1969. 22 pages.
TWI 3-A12. Fluorometric procedures for dye tracing, Revised, by James F. Wilson, Jr., Ernest D. Cobb, and Frederick A. Kilpatrick. 1986. 41 pages.
TWI 3-A13. Computation of continuous records of streamflow, by Edward J. Kennedy. 1983. 53 pages.
TWI 3-A14. Use of flumes in measuring discharge, by F.A. Kilpatrick, and V.R. Schneider. 1983. 46 pages.
TWI 3-A15. Computation of water-surface profiles in open channels, by Jacob Davidian. 1984. 48 pages.
TWI 3-A16. Measurement of discharge using tracers, by F.A. Kilpatrick and E.D. Cobb. 1985. 52 pages.
TWI 3-A17. Acoustic velocity meter systems, by Antonius Laenen. 1985. 38 pages.
TWI 3-B1. Aquifer-test design, observation, and data analysis, by R.W. Stallman. 1971. 26 pages.
TWI 3-B2.[1] Introduction to ground-water hydraulics, a programmed text for self-instruction, by G.D. Bennett. 1976. 172 pages.
TWI 3-B3. Type curves for selected problems of flow to wells in confined aquifers, by J.E. Reed. 1980. 106 pages.
TWI 3-B5. Definition of boundary and initial conditions in the analysis of saturated ground-water flow systems—an introduction, by O. Lehn Franke, Thomas E. Reilly, and Gordon D. Bennett. 1987. 15 pages.
TWI 3-B6. The principle of superposition and its application in ground-water hydraulics, by Thomas E. Reilly, O. Lehn Franke, and Gordon D. Bennett. 1987. 28 pages.
TWI 3-C1. Fluvial sediment concepts, by H.P. Guy. 1970. 55 pages.
TWI 3-C2. Field methods of measurement of fluvial sediment, by H.P. Guy and V.W. Norman. 1970. 59 pages.
TWI 3-C3. Computation of fluvial-sediment discharge, by George Porterfield. 1972. 66 pages.
TWI 4-A1. Some statistical tools in hydrology, by H.C. Riggs. 1968. 39 pages.
TWI 4-A2. Frequency curves, by H.C. Riggs, 1968. 15 pages.
TWI 4-B1. Low-flow investigations, by H.C. Riggs. 1972. 18 pages.
TWI 4-B2. Storage analyses for water supply, by H.C. Riggs and C.H. Hardison. 1973. 20 pages.
TWI 4-B3. Regional analyses of streamflow characteristics, by H.C. Riggs. 1973. 15 pages.
TWI 4-D1. Computation of rate and volume of stream depletion by wells, by C.T. Jenkins. 1970. 17 pages.

[1]Spanish translation also available.

TWI 5-A1. Methods for determination of inorganic substances in water and fluvial sediments, by M.W. Skougstad and others, editors. 1979. 626 pages.

TWI 5-A2. Determination of minor elements in water by emission spectroscopy, by P.R. Barnett and E.C. Mallory, Jr. 1971. 31 pages.

TWI 5-A3. Methods for the determination of organic substances in water and fluvial sediments, edited by R.L. Wershaw, M.J. Fishman, R.R. Grabbe, and L.E. Lowe. 1987. 80 pages. This manual is a revision of "Methods for Analysis of Organic Substances in Water" by Donald F. Goerlitz and Eugene Brown, Book 5, Chapter A3, published in 1972.

TWI 5-A4. Methods for collection and analysis of aquatic biological and microbiological samples, edited by P.E. Greeson, T.A. Ehlke, G.A. Irwin, B.W. Lium, and K.V. Slack. 1977. 332 pages.

TWI 5-A5. Methods for determination of radioactive substances in water and fluvial sediments, by L.L. Thatcher, V.J. Janzer, and K.W. Edwards. 1977. 95 pages.

TWI 5-A6. Quality assurance practices for the chemical and biological analyses of water and fluvial sediments, by L.C. Friedman and D.E. Erdmann. 1982. 181 pages.

TWI 5-C1. Laboratory theory and methods for sediment analysis, by H.P. Guy. 1969. 58 pages.

TWI 6-A1. A modular three-dimensional finite-difference ground-water flow model, by Michael G. McDonald and Arlen W. Harbaugh. 1988. 586 pages.

TWI 7-C1. Finite difference model for aquifer simulation in two dimensions with results of numerical experiments, by P.C. Trescott, G.F. Pinder, and S.P. Larson. 1976. 116 pages.

TWI 7-C2. Computer model of two-dimensional solute transport and dispersion in ground water, by L.F. Konikow and J.D. Bredehoeft. 1978. 90 pages.

TWI 7-C3. A model for simulation of flow in singular and interconnected channels, by R.W. Schaffranek, R.A. Baltzer, and D.E. Goldberg. 1981. 110 pages.

TWI 8-A1. Methods of measuring water levels in deep wells, by M.S. Garber and F.C. Koopman. 1968. 23 pages.

TWI 8-A2. Installation and service manual for U.S. Geological Survey monometers, by J.D. Craig. 1983. 57 pages.

TWI 8-B2. Calibration and maintenance of vertical-axis type current meters, by G.F. Smoot and C.E. Novak. 1968. 15 pages.

CONTENTS

Page

Abstract ---- 1
Introduction ---- 1
Purpose and scope ---- 2
Surface geophysical techniques in hydrologic studies ---- 2
References ---- 2
Seismic-refraction theory and limitations ---- 3
Theory ---- 3
Interpretation formulas ---- 3
Two-layer parallel-boundary formulas ---- 4
Three-layer parallel-boundary formulas ---- 4
Two-layer dipping-boundary formulas ---- 5
Example problem ---- 9
Multilayer dipping-boundary formulas ---- 13
Formulas for more complex cases ---- 13
Field corrections ---- 13
Summary ---- 13
Limitations ---- 13
Thin, intermediate-seismic-velocity refractor ---- 13
Example problem ---- 14
Insufficient seismic-velocity contrasts between hydrogeologic units ---- 16
Low-seismic-velocity units underlying high-seismic-velocity units ---- 16
Example problem ---- 18
Other limitations of seismic-refraction techniques ---- 19
Ambient noise ---- 19
Horizontal variations in the velocity of sound and the thickness of the weathered zone ---- 19
Accuracy of seismic-refraction measurements ---- 19
Annotated references ---- 20
Applications of seismic-refraction techniques to hydrology ---- 22
Hydrogeologic settings in which seismic-refraction techniques can be used successfully ---- 22
Unconsolidated unsaturated glacial or alluvial material overlying glacial or alluvial aquifers ---- 22
Unconsolidated glacial or alluvial material overlying consolidated bedrock ---- 23
Thick, unconsolidated alluvial or sedimentary materials overlying consolidated sediments and (or) basement rock in large structural basins ---- 24
Unconsolidated alluvial material overlying sedimentary rock, which in turn overlies volcanic or crystalline bedrock ---- 24
Unconsolidated stratified-drift material overlying significant deposits of dense lodgement glacial till, which in turn overlie crystalline bedrock ---- 26
Hydrogeologic settings in which seismic-refraction techniques may work, but with difficulty ---- 26
Unconsolidated glacial sand and gravel overlying a thin till layer, which in turn overlies crystalline bedrock ---- 29
An aquifer underlain by bedrock having a similar seismic velocity ---- 30
A study area having a surface layer that varies significantly in thickness or material composition ---- 30

Page

Applications of seismic-refraction techniques to hydrology—Continued
Hydrogeologic settings in which seismic-refraction techniques may work, but with difficulty—Continued
Quantitative estimation of aquifer hydraulic properties ---- 31
Ground-water contamination in unconsolidated materials ---- 34
A multilayered Earth with a shallow, thin layer that has a seismic velocity greater than the layers below it ---- 35
Miscellaneous hydrogeologic settings ---- 35
Hydrogeologic settings in which seismic-refraction techniques cannot be used ---- 35
Basalt flows with interflow zones that are aquifers ---- 35
Unconsolidated sand and gravel aquifer material underlain by silt and clay ---- 35
Saturated alluvium underlain by a thin confining shale, which in turn overlies a porous sandstone ---- 37
Annotated references ---- 37
Unconsolidated unsaturated glacial or alluvial material overlying glacial or alluvial aquifers ---- 37
Unconsolidated glacial or alluvial material overlying consolidated bedrock ---- 37
Thick unconsolidated alluvial or sedimentary material overlying consolidated sediments and (or) basement rock in large structural basins ---- 37
Unconsolidated alluvial material overlying sedimentary rock, which in turn overlies volcanic or crystalline bedrock ---- 38
Unconsolidated stratified-drift material overlying significant deposits of dense lodgement glacial till, which in turn overlie crystalline bedrock ---- 38
Unconsolidated glacial sand and gravel overlying a thin till layer, which in turn overlies crystalline bedrock ---- 38
An aquifer unit underlain by bedrock having a similar seismic velocity ---- 39
A study area having a surface layer that varies significantly in thickness or material composition ---- 39
Quantitative estimation of aquifer hydraulic properties ---- 39
Ground-water contamination in unconsolidated materials ---- 40
A multilayered Earth with a shallow, thin layer that has a seismic velocity greater than the layers below it ---- 40
Miscellaneous hydrogeologic settings ---- 40
Unconsolidated sand and gravel aquifer material underlain by silt and clay ---- 40
Saturated alluvium underlain by a thin confining shale, which in turn overlies a porous sandstone ---- 40
Planning the investigation ---- 40
Local geology ---- 41
Available data ---- 41

	Page
Planning the investigation—Continued	
Seismic velocities	42
Objective of the seismic-refraction survey	42
Site selection	42
Summary	44
References	44
Equipment	45
Seismograph	45
Geophones	45
Geophone cables	45
Energy sources	47
Shot cables	50
Portable radios	51
Field vehicles	51
Levels and transits	53
Miscellaneous tools	53
References	53
Field procedures	53
Reconnaissance refraction survey of a site	53
Field interpretation and calculations	53
Example problem	54
Quantity or quality of field data	56
Example problem	60
Field crew	60
Field records	66
References	69
Interpretation techniques	69
Seismograph records	69
Time-distance plots	69
Manual interpretation techniques	72
Computer-assisted interpretation techniques	72
Formulas	72
Modeling techniques	72
References	85

FIGURES

		Page
1–14.	Diagrams showing:	
	1. Raypaths of refracted and reflected sound energy in a two-layer Earth	4
	2. Seismic wave fronts and raypaths and corresponding time-distance plot	5
	3. Seismic raypaths and time-distance plot for a two-layer model with parallel boundaries	6
	4. Seismic raypaths and time-distance plot for a three-layer model with parallel boundaries	7
	5. Seismic raypaths and time-distance plot for a two-layer model with a dipping boundary	8
	6. Time-distance plot resulting from one shotpoint over a two-layer model with a dipping boundary	10
	7. Time-distance plot resulting from two reversed shots over a two-layer model with a dipping boundary	11
	8. Advantages and disadvantages of intercept-time versus crossover-distance formulas in determining depth to a refractor under different field conditions	12
	9. Seismic wave fronts with selected raypaths and the corresponding time-distance plot for the case of an undetectable intermediate-seismic-velocity layer	14
	10. Time-distance plot showing two layers in an area known to have three layers	15
	11. Seismic section with hidden layer and resulting time-distance plot	17
	12. Seismic section with velocity reversal and resulting time-distance plot	18
	13. Interpreted seismic section and time-distance plot for a four-layer model having frozen ground at the surface	20
	14. Time-distance plot and interpreted seismic section from a ground-water study in Vertessomto, Hungary	23
15.	Generalized location map of Great Swamp National Wildlife Refuge, N.J., and location of seismic-refraction profile A-A′	24
16.	Diagram showing time-distance plot and interpreted seismic section near Great Swamp National Wildlife Refuge, Morristown, N.J.	25
17.	Generalized location map of Aura-Altar basin, Arizona, and location of seismic-refraction profile A-A′	26
18.	Diagram showing interpreted seismic section A-A′ in Aura-Altar basin, near Tucson, Ariz.	27
19.	Generalized location map of central Guanajibo Valley, Puerto Rico, and location of seismic-refraction profile A-A′	28
20.	Diagram showing time-distance plot and interpreted seismic section at Guanajibo Valley, Puerto Rico	29
21.	Generalized location map of Farmington, Conn., and location of seismic-refraction profile A-A′	30
22.	Diagram showing time-distance plot and interpreted seismic section near Farmington, Conn.	31
23.	Map showing saturated thickness of stratified drift and location of seismic-refraction lines in the Pootatuck River valley, Newtown, Conn.	32
24–26.	Diagrams showing:	
	24. Time-distance plot and interpreted seismic section of Pootatuck River valley, Newtown, Conn.	33
	25. Hypothetical time-distance plots resulting from different seismic velocities in the second layer	34
	26. Seismic section with shallow seismic-velocity discontinuities and relief on a refracting surface, and the resulting time-distance plot, Monument Valley area of Arizona and Utah	34
27.	Site diagram and seismic section of a sanitary landfill in Farmington, Conn.	36
28.	Schematic diagram of a typical seismic-refraction system	45
29.	Seismograms showing improvement in first breaks by stacking successive hammer impacts: 1 impact, 5 impacts, and 10 impacts	46
30.	Photograph of a typical 12-channel seismograph	47
31.	Photographs and diagrams of commonly used geophone, breast reel, geophone cables, and geophone extension cable	48

ABBREVIATIONS AND CONVERSION FACTORS

Factors for converting inch-pound units to International System of Units (SI) and abbreviation of units:

Multiply inch-pound unit	*By*	*To obtain SI (metric) unit*
	Length	
foot (ft)	0.3048	meter (m)
mile (mi)	1.609	kilometer (km)
	Velocity	
foot per second (ft/s)	0.3048	meter per second (m/s)
	Density	
ounce per cubic inch (oz/in^3)	1.7297	gram per cubic centimeter (g/cm^3)

GLOSSARY

Angle of incidence. The acute angle between a raypath and the normal to an interface.

Apparent velocity. The velocity at which a fixed point on a seismic wave, usually its front or beginning, passes an observer.

Blind zone. A layer having lower seismic velocity than overlying layers so that it does not carry a head wave.

Conductivity. The property of a material that allows the flow of electrical current.

Critical angle. The angle of incidence at which a refracted ray just grazes the interface between two media having different seismic velocities; equal to $\sin^{-1} V_1/V_2$.

Critical distance. The offset at which reflection occurs at the critical angle.

Crossover distance. The source-to-receiver distance at which refracted waves following a deep high-speed marker overtake direct waves, or refracted waves, following shallower markers.

Geophone spacing. The distance between adjacent geophones within a spread.

Geophone spread. The arrangement of geophones in relation to the position of the energy source.

Head wave. A wave characterized by entering and leaving a high-velocity medium at the critical angle.

Isotropic. A substance that has the same physical properties regardless of the direction of measurement.

Reflection. Energy from a seismic source that has been reflected from an acoustic impedence contrast between layers within the Earth.

Resistivity. The property of a material that inhibits the flow of electrical current. Resistivity is the reciprocal of conductivity.

Stack. A composite seismic record made by combining traces from different shots.

Unconsolidated. Loose material of the Earth's surface; uncemented particles of solid matter.

Weathered layer. Zone near the Earth's surface characterized by a low seismic-wave velocity beneath which the velocity abruptly increases, more properly called the low-velocity layer.

Page

32. Photographs of commonly used seismic energy sources: shotgun, sledge hammer, explosives, and weight drop ---- 49
33. Photograph showing the mixing of two-component explosives in the field ---- 50
34. Diagram showing use of safety wire in explosive-firing circuit ---- 51
35. Photographs of van and pickup truck used for seismic-refraction fieldwork ---- 52
36–44. Diagrams showing:
36. Time-distance plot and interpreted seismic section for a three-layer problem ---- 55
37. Time-distance plots and field setups used to determine the seismic velocities in a three-layer problem ---- 57
38. Field setup of shotpoints and geophones for delineation of multiple-refracting horizons ---- 58
39. Time-distance plot and interpreted seismic section resulting from a single geophone spread with five shotpoints ---- 58
40. Time-distance plot and interpreted seismic section resulting from a single geophone spread with two shotpoints ---- 59
41. Shotpoint and geophone geometries for various thicknesses and depths of layer 2 and the resulting time-distance plots ---- 62
42. Field setup of seismic truck, geophones, and shot hole ---- 64
43. Assembly of explosive cartridges and electric blasting caps ---- 65
44. Various field setups and resulting time-distance and depth plots for each geophone in a two-layer problem ---- 67
45. Data sheet for recording field data ---- 68
46, 47. Photographs of:
46. A 12-channel analog seismograph record showing good first breaks produced by an explosive sound source ---- 70
47. A 12-channel digital seismograph record from Little Androscoggin River valley, Maine, showing sharp first breaks produced by an explosive sound source in an area with low background noise ---- 70
48, 49. Seismograph records with—
48. Rounded first breaks produced by a sledge-hammer sound source in an area with high background noise ---- 71
49. Sharp first breaks produced by an explosive sound source in an area with high background noise ---- 71
50, 51. Diagrams showing:
50. Reversed seismic-refraction profiles with two velocity layers depicted on the time-distance plot ---- 72
51. Relationships between field setup, time-distance plot, and interpreted seismic section ---- 74
52. Data sheet for recording first-arrival times and other seismic information ---- 76
53. Diagrams showing shotpoint and geophone locations and altitudes plotted to scale ---- 77
54. Example of data input form for entering data in the interactive version of the Seismic Interpretation Program (SIPT) ---- 78
55–59. Diagrams showing:
55. Effect of topographic relief on raw and datum-corrected time-distance plots ---- 79
56. Common errors indicated by unusual time-distance plots ---- 80
57. Seismic section and time-distance plot showing the general relationships of seismic-layer velocities and crossover distances between three seismic-refraction spreads ---- 81
58. Effects of incorrect layer assignments on the velocity of sound as computed by regression in the Seismic Interpretation Program (SIPT) ---- 83
59. Good and poor computer-aided interpretations of seismic-refraction data ---- 84

TABLES

Page

1. Maximum thickness of an undetectable layer in various hydrogeologic settings ---- 16
2. Comparison of the depth to water determined by seismic-refraction methods and by drilling ---- 23
3. Compressional velocity of sound in common Earth materials ---- 41
4. Laboratory-determined physical properties of sedimentary rock samples from south-central Connecticut ---- 43
5. Field-determined compressional velocity of sound in shallow, saturated unconsolidated deposits ---- 44
6. Advantages and limitations of seismic-refraction energy sources ---- 47
7. Typical field-crew work assignments for seismic studies ---- 61
8. Probability of hazardous flying rock debris resulting from use of different quantities of explosives under different field conditions ---- 64
9. Example of input data set for the Seismic Interpretation Program (SIPT) ---- 82

APPLICATION OF SEISMIC-REFRACTION TECHNIQUES TO HYDROLOGIC STUDIES

By F.P. Haeni

Abstract

During the past 30 years, seismic-refraction methods have been used extensively in petroleum, mineral, and engineering investigations and to some extent for hydrologic applications. Recent advances in equipment, sound sources, and computer interpretation techniques make seismic refraction a highly effective and economical means of obtaining subsurface data in hydrologic studies. Aquifers that can be defined by one or more high-seismic-velocity surface, such as (1) alluvial or glacial deposits in consolidated rock valleys, (2) limestone or sandstone underlain by metamorphic or igneous rock, or (3) saturated unconsolidated deposits overlain by unsaturated unconsolidated deposits, are ideally suited for seismic-refraction methods. These methods allow economical collection of subsurface data, provide the basis for more efficient collection of data by test drilling or aquifer tests, and result in improved hydrologic studies.

This manual briefly reviews the basics of seismic-refraction theory and principles. It emphasizes the use of these techniques in hydrologic investigations and describes the planning, equipment, field procedures, and intrepretation techniques needed for this type of study. Furthermore, examples of the use of seismic-refraction techniques in a wide variety of hydrologic studies are presented.

Introduction

Surface geophysical techniques have been used extensively in the petroleum, mineral, and engineering fields. Hydrologic investigations have used surface geophysical techniques in the past, but to only a limited degree. Recent advances in electronic equipment and computer-interpretation programs and the development of new techniques make surface geophysics a more effective tool for hydrologists. These techniques should be considered in the project planning process and used where appropriate. Treated as a tool, similar to pump tests, simulation modeling, test drilling, geologic maps, borehole geophysical techniques, and so forth, these techniques can be used to help solve hydrologic problems.

Classically, surface geophysical techniques have been used early in the exploration process, prior to use of more expensive data-collection techniques such as drilling (Jakosky, 1950). The use of surface geophysics in this manner minimizes expensive data-collection activities and results in more efficient hydrologic studies.

All surface geophysical methods measure some physical property of subsurface materials or fluids. Selection of the appropriate geophysical method is determined by the specific physical property of a hydrologic unit or by the differences between adjacent hydrologic units. Typical physical properties measured are electrical resistivity, electrical conductivity, velocity of sound, gravity fields, and magnetic fields. Knowledge of the physical properties of a subsurface material is critical for successful application of surface geophysical methods. Aquifers that can be defined by one or more high-seismic-velocity surfaces, such as alluvial or glacial deposits in consolidated rock valleys, limestone or sandstone underlain by metamorphic or igneous rock, or saturated unconsolidated deposits overlain by unsaturated unconsolidated deposits, are ideally suited for seismic-refraction methods. In these hydrogeologic settings, seismic-refraction methods have proved to be the most useful of the surface geophysical techniques (Grant and West, 1965).

Seismic-refraction techniques were among the first geophysical tools used in the exploration for petroleum. In the 1920's, these techniques helped find many structures that were associated with petroleum accumulations. With the introduction and refinement of seismic-reflection techniques during the 1930's, use of refraction methods by the petroleum industry declined, and they are now used primarily in special situations and for weathered-layer velocity determinations.

Use of seismic-refraction techniques in engineering and hydrologic applications, and in coal exploration, has increased over the years, as has the wealth of literature on interpretation procedures. A bibliography by Musgrave (1967, p. 565–594) shows the extent of interest in, and the variety of applications of, seismic-refraction techniques.

Although seismic-reflection techniques have dominated deep-exploration work in recent years, shallow-exploration work has used seismic-refraction techniques

extensively. Advances in the miniaturization of electronic equipment and the use of computers for data interpretation have made seismic-refraction techniques a very effective and economical exploration tool for hydrologists.

Purpose and scope

A brief review of the literature indicates the diversity of seismic-refraction techniques. The purpose of this manual is to help the hydrologist who wishes to apply seismic refraction to a particular project or area of interest. It is intended to help the hydrologist determine if seismic-refraction techniques will work in a particular hydrologic setting. In addition, the manual briefly presents the theory of seismic refraction, identifies advantages and limitations of the techniques, describes the equipment and general field procedures required, and presents several interpretation procedures. Numerous references are cited to provide the reader with additional sources of information which are beyond the scope of this manual.

The techniques presented here are not standardized or rigid, but they have been used effectively in a wide variety of hydrologic studies conducted by the U.S. Geological Survey and others. References are included with each section so that alternative approaches to field procedures and interpretation methods can be investigated.

Ultimately, success in using seismic-refraction methods will depend more on the ability of the hydrologist to apply the principles of the techniques and to extract a hydrologically reasonable answer than on the use of a particular method of interpretation.

Surface geophysical techniques in hydrologic studies

Surface geophysical techniques are used to obtain information about the subsurface units that control the location and movement of ground water.

A standard approach in exploration investigations is first to assess geologic conditions from available surface and subsurface geological data. From this initial study, the regional or local geologic framework can be hypothesized and the magnitude of the exploration problem defined.

At this point in a study, surface geophysical methods can be used to great advantage. The geologic and hydrologic model developed in this first stage of the study from scattered data points can be verified or, if necessary, modified. The importance of the interdependence of geological data, hydrologic data, and geophysical data cannot be overemphasized. Geophysical data by itself is susceptible to many interpretations. The input of hydrologic or geologic constraints may eliminate unreasonable interpretations and result in the selection of a unique solution.

Commonly, one or more surface geophysical techniques can be used advantageously in a hydrologic investigation. Papers describing the use of individual and combined surface geophysical techniques in hydrologic studies include those of Bonini and Hickok (1958), Eaton and Watkins (1967), Lennox and Carlson (1967), Mabey (1967), Ogiluy (1967), Shiftan (1967), Kent and Sendlein (1972), Zohdy and others (1974), Worthington (1975), and Collett (1978).

The two types of surface geophysical techniques that have been used most widely in hydrologic studies are resistivity methods and seismic-refraction methods. The general use of seismic-refraction methods in hydrologic studies has been discussed in the literature, and in cases in which velocity discontinuities between hydrologic units are present, these methods have proved to be the most useful geophysical technique. The major use of seismic-refraction techniques in hydrologic studies is to assess the hydrogeologic framework and hydrologic boundaries of aquifers. They are generally used early in the investigation, after the preliminary hydrologic assessment and prior to more site-specific data-gathering activities. Another use is for specific data-gathering activities later in the study. Specific information that may be sought during the hydrologic analysis stage of the study, and that can be investigated by seismic-refraction methods, are the depth to water in unconsolidated aquifers at specific locations and the location of aquifer boundaries.

After the geophysical work, the study is ready to enter its final stages when more costly, detailed site-specific data are collected. Generally, these stages of the study involve a drilling program, borehole geophysical studies, detailed hydrologic testing, and data analysis.

References

Bonini, W.E., and Hickok, E.A., 1958, Seismic refraction method in ground-water exploration: Transactions of the American Institute of Mining, Metallurgical, and Petroleum Engineers, v. 211, p. 485–488.

Collett, L.S., 1978, Introduction to hydrogeophysics: Conference of the International Association of Hydrogeologists, Canadian chapter, Edmonton, September 30-October 4, 1978, Proceedings, p. 16–35.

Eaton, G.P., and Watkins, J.S., 1967, The use of seismic refraction and gravity methods in hydrologic investigations, *in* Morey, L.W., ed., Mining and ground-water geophysics: Geological Survey of Canada Economic Geology Report 26, p. 554–568.

Grant, F.S., and West, G.F., 1965, Interpretation theory in applied geophysics: New York, McGraw Hill, 583 p.

Jakosky, J.J., 1950, Exploration geophysics (2d ed.): Los Angeles, Calif., Times-Mirror Press, 1,195 p.

Kent, D.C., and Sendlein, L.V.A., 1972, A basin study of ground-water discharge from bedrock into glacial drift: Part 1, Definition of ground-water systems: Ground Water, v. 10, no. 4, p. 24–34.

Lennox, D.H., and Carlson, V., 1967, Integration of geophysical methods for ground-water exploration in the prairie provinces, Canada, *in* Morey, L.W., ed., Mining and ground-water geophysics: Geological Survey of Canada Economic Geology Report 26, p. 517–535.

Mabey, D.R., 1967, The role of geophysics in the development of the World's ground-water resources, *in* Morey, L.W., ed., Mining and ground-water geophysics: Geological Survey of Canada Economic Geology Report 26, p. 267–271.

Musgrave, A.W., ed., 1967, Seismic refraction prospecting: Tulsa, Okla., Society of Exploration Geophysicists, 604 p.

Ogiluy, A.A., 1967, Geophysical prospecting for ground water in the Soviet Union, *in* Morey, L.W., ed., Mining and ground-water geophysics: Geological Survey of Canada Economic Geology Report 26, p. 536–543.

Shiftan, Z.L., 1967, Integration of geophysics and hydrogeology in the solution of regional ground-water problems, *in* Morey, L.W., ed., Mining and ground-water geophysics: Geological Survey of Canada Economic Geology Report 26, p. 507–516.

Worthington, P.A., 1975, Procedures for the optimum use of geophysical methods in ground-water development programs: Association of Engineering Geologists Bulletin, v. 12, no. 1, p. 23–38.

Zohdy, A.A.R., Eaton, G.P., and Mabey, D.R., 1974, Application of surface geophysics to ground-water investigations: U.S. Geological Survey Techniques of Water-Resources Investigations, Book 2, Chapter D1, 116 p.

Seismic-Refraction Theory and Limitations

Theory

Numerous textbooks and journal articles present the details of seismic-refraction theory (Slotnick, 1959; Grant and West, 1965; Griffiths and King, 1965; Musgrave, 1967; Dobrin, 1976; Telford and others, 1976; Parasnis, 1979; Mooney, 1981). The following discussion reviews only the basic principles and limitations of seismic-refraction methods. The annotated bibliography at the end of this section should be used by hydrologists not familiar with seismic theory to select one or more publications that clearly present a rigorous theoretical development. An encyclopedic dictionary of terms used in exploration geophysics is published by the Society of Exploration Geophysicists (Sheriff, 1973).

It must be emphasized that the absence of an extensive section on the theory of seismic refraction does not minimize the importance of the topic. Hydrologists unfamiliar with geophysics must have a solid understanding of the physics underlying the technique prior to using it.

Seismic-refraction methods measure the time it takes for a compressional sound wave generated by a sound source to travel down through the layers of the Earth and back up to detectors placed on the land surface (fig. 1). By measuring the traveltime of the sound wave and applying the laws of physics that govern the propagation of sound, the subsurface geology can be inferred. The field data, therefore, will consist of measured distances and seismic traveltimes. From this time-distance information, velocity variations and depths to individual layers can be calculated and modeled.

The foundation of seismic-refraction theory is Snell's Law, which governs the refraction of sound or light waves across the boundary between layers having different velocities. As sound propagates through one layer and encounters another layer having faster seismic velocities, part of the energy is refracted, or bent, and part is reflected back into the first layer (see raypath 1 in fig. 1). When the angle of incidence equals the critical angle, the compressional energy is transmitted along the upper surface of the second layer at the velocity of sound in the second layer (see raypath 2 in fig. 1). As this energy propagates along the surface of layer 2, it generates new sound waves in the upper medium according to Huygens' principle, which states that every point on an advancing wave front can be regarded as the source of a sound wave; these new sound waves propagate back to the surface through layer 1 at an angle equal to the critical angle and at the velocity of sound in layer 1. When this refracted wave arrives at the land surface, it activates a geophone and arrival energy is recorded on a seismograph.

If a series of geophones is spread out on the ground in a geometric array, arrival times can be plotted against source-to-geophone distances (fig. 2), which results in a time-distance plot, or time-distance curve. It can be seen from figure 2 that at any distance less than the crossover distance (x_c) (sometimes incorrectly called the critical distance), the sound travels directly from the source to the detectors. This compressional wave travels a known distance in a known time, and the velocity of layer 1 can be directly calculated by $V_1 = x/t$, where V_1 is the velocity of sound in layer 1 and x is the distance a wave travels in layer 1 in time t. Figure 2 is a plot of time as a function of distance; consequently, V_1 is also equal to the inverse slope of the first line segment.

Beyond the crossover distance, the compressional wave that has traveled through layer 1, along the interface with the high-velocity layer, and then back up to the surface through layer 1 arrives before the compressional wave that has been in layer 1 (the low-velocity layer). All first compressional waves arriving at geophones more distant than the crossover distance will be refracted waves, or head waves, from layer 2 (the high-velocity layer). When these points are plotted on the time-distance plot, the inverse slope of this segment will be equal to the apparent velocity of layer 2. The slope of this line does not intersect the time axis at zero, but at some time called the intercept time (t_i). The intercept time and the crossover distance are directly dependent on the velocity of sound in the two materials and the thickness of the first layer, and therefore can be used to determine the thickness of the first layer (z).

Interpretation formulas

Intercept times and crossover distance-depth formulas have been derived in the literature (Grant and West, 1965; Zohdy and others, 1974; Dobrin, 1976; Telford and

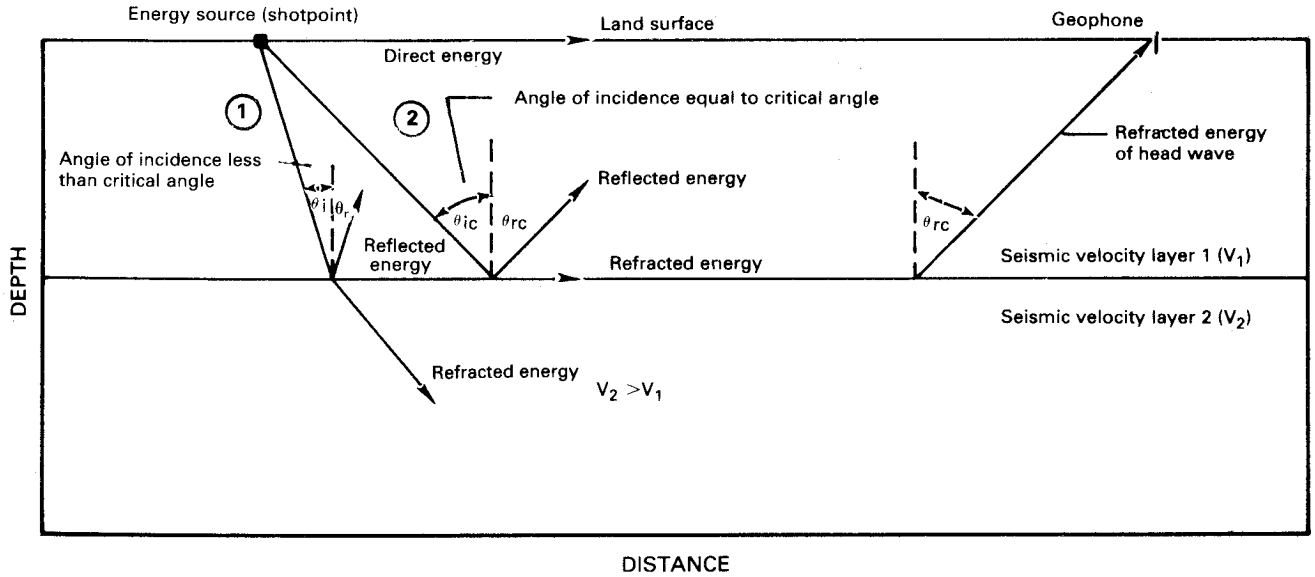

Figure 1.—Raypaths of refracted (1) and reflected (2) sound energy in a two-layer Earth.

others, 1976; Parasnis, 1979; Mooney, 1981), and only the results are given here. These derivations are straightforward inasmuch as the total traveltime of the sound wave is measured, the velocity in each layer is calculated from the time-distance plot, and the raypath geometry is known. The only unknown is the depth to the high-velocity refractor. These interpretation formulas are based on the following assumptions: (1) the boundaries between layers are planes that are either horizontal or dipping at a constant angle, (2) there is no land-surface relief, (3) each layer is homogeneous and isotropic, and (4) the seismic velocity of the layers increases with depth.

Two-layer parallel-boundary formulas (See figure 3)

1. Intercept-time formula (Dobrin, 1976, p. 297):

$$z=\frac{t_i}{2}\frac{V_2 V_1}{\sqrt{(V_2)^2-(V_1)^2}}, \qquad (1)$$

where

z = depth to layer 2 at point,
t_i = intercept time,
V_2 = velocity of sound in layer 2, and
V_1 = velocity of sound in layer 1.

2. Crossover-distance formula (Dobrin, 1976, p. 298):

$$z=\frac{x_c}{2}\sqrt{\frac{V_2-V_1}{V_2+V_1}}, \qquad (2)$$

where

z, V_2, and V_1 are as defined earlier and
x_c = crossover distance.

Three-layer parallel-boundary formulas (See figure 4)

1. Intercept-time formulas (Dobrin, 1976, p. 299):

$$z_1=\frac{t_2}{2}\frac{V_2V_1}{\sqrt{(V_2)^2-(V_1)^2}} \text{ (from two-layer formula 1)}, \qquad (3)$$

$$z_2=\frac{1}{2}\left(t_3-\frac{2z_1\sqrt{(V_3)^2-(V_1)^2}}{V_3V_1}\right)\frac{V_3V_2}{\sqrt{(V_3)^2-(V_2)^2}}, \qquad (4)$$

and

$$z_3=z_1+z_2, \qquad (5)$$

where

z_1 = depth to layer 2, or thickness of layer 1,
z_2 = depth from bottom of layer 1 to top of layer 3, or thickness of layer 2,
z_3 = depth from surface to top of layer 3,
t_2 = intercept time for layer 2,
t_3 = intercept time for layer 3,
V_1 = velocity of sound in layer 1,
V_2 = velocity of sound in layer 2, and
V_3 = velocity of sound in layer 3.

2. Crossover-distance formulas (Parasnis, 1979, p. 197–198):

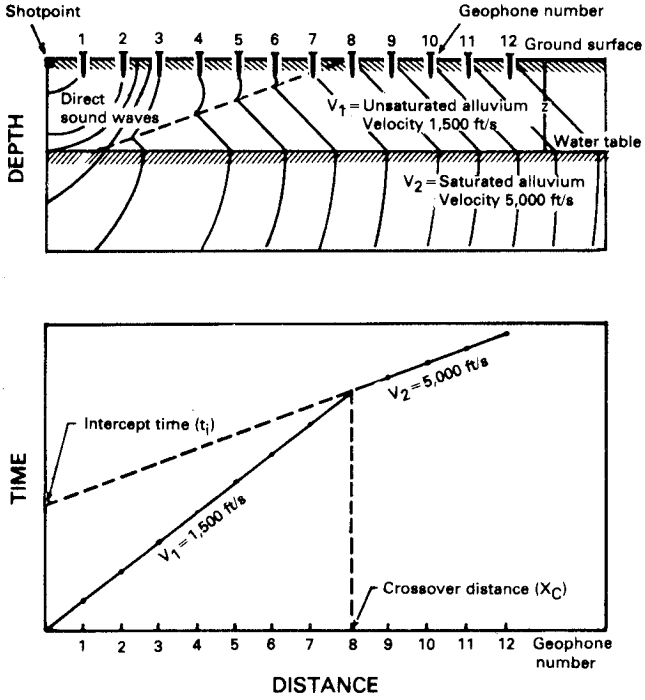

Figure 2.—Seismic wave fronts and raypaths and corresponding time-distance plot.

$$z_1=\frac{x_{c1}}{2}\sqrt{\frac{V_2-V_1}{V_2+V_1}} \text{ (from two-layer formula 2),} \quad (6)$$

$$z_2=\frac{x_{c2}}{2}\left(\frac{V_3-V_2}{\sqrt{(V_3)^2-(V_2)^2}}\right)$$

$$-z_1\left(\frac{V_2\sqrt{(V_3)^2-(V_1)^2}-V_3\sqrt{(V_2)^2-(V_1)^2}}{V_1\sqrt{(V_3)^2-(V_2)^2}}\right), \quad (7)$$

and

$$z_3=z_1+z_2\,, \quad (8)$$

where

z_1, z_2, z_3, V_1, V_2, and V_3 are as defined earlier,
x_{c1} = crossover distance between layers 1 and 2, and
x_{c2} = crossover distance between layers 2 and 3.

Other forms of this equation are presented by Mooney (1981) and Alsop (1982).

Two-layer dipping-boundary formulas (See figure 5)

The problem presented by a dipping boundary between layers adds some geometric complexity to the derivation of these formulas. Several important concepts of seismic-refraction theory must be introduced at this point.

To learn about the geometry of a dipping boundary, the refraction profile must be reversed. For a single array, a minimum of two shots must be fired, one from each end of the array. This concept is termed "reversed-profile shooting," and the practice should be followed routinely in all seismic-refraction studies. Failure to reverse seismic profiles leads to invalid results in almost all situations. Figure 5 shows a two-layer dipping-boundary model and the resultant time-distance plot. A fundamental rule of seismic-refraction theory is illustrated in figure 5. The total traveltime of compressional sound waves from shotpoint D to shotpoint U, and in the opposite direction, from shotpoint U to shotpoint D, must be equal; that is, T_u must equal T_d because the same wave path is followed in each case. Comparison of the crossover distances or the intercept times on this plot ($x_{cu} > x_{cd}$ and $t_{2u} > t_{2d}$) shows that layer 2 is deeper at shotpoint 2 than at shotpoint 1, and a dipping-layer analysis must be used. If these values were equal and the segments of the time-distance plots were straight lines, then simple two-layer parallel-boundary formulas could be used.

In the parallel-boundary problems discussed previously, the seismic velocity measured on time-distance plots was in fact the true velocity of the horizontal refracting layer. When the interface is dipping, however, seismic-refraction methods measure the apparent seismic velocity and not the true seismic velocity. The true seismic velocity is the harmonic mean of the measured apparent updip and downdip velocities multiplied by the cosine of the dip angle. It can be determined by the following formula:

$$V_2=\frac{2V_{2u}V_{2d}}{V_{2u}+V_{2d}}\cos\xi \text{ (Redpath, 1973; Mooney, 1981, p. 10–4),} \quad (9)$$

where

V_2 = true velocity of sound in layer 2,
V_{2u} = apparent updip velocity of sound (from time-distance plot),
V_{2d} = apparent downdip velocity of sound (from time-distance plot), and
ξ = dip angle of layer 2.

A good approximation of the velocity of sound in layer 2 is the harmonic mean, since the cosine of small angles is very close to 1.0. Equation 9 reduces to

$$V_2=\frac{2V_{2u}V_{2d}}{V_{2u}+V_{2d}} \text{ (Redpath, 1973, p. 9).} \quad (10)$$

The depth to the dipping interface can be calculated by using the following formulas:

1. Intercept-time formulas (Dobrin, 1976, p. 304):

$$\text{(a)} \quad \theta_c=\tfrac{1}{2}\left(\sin^{-1} V_1m_d+\sin^{-1} V_1m_u\right), \quad (11)$$

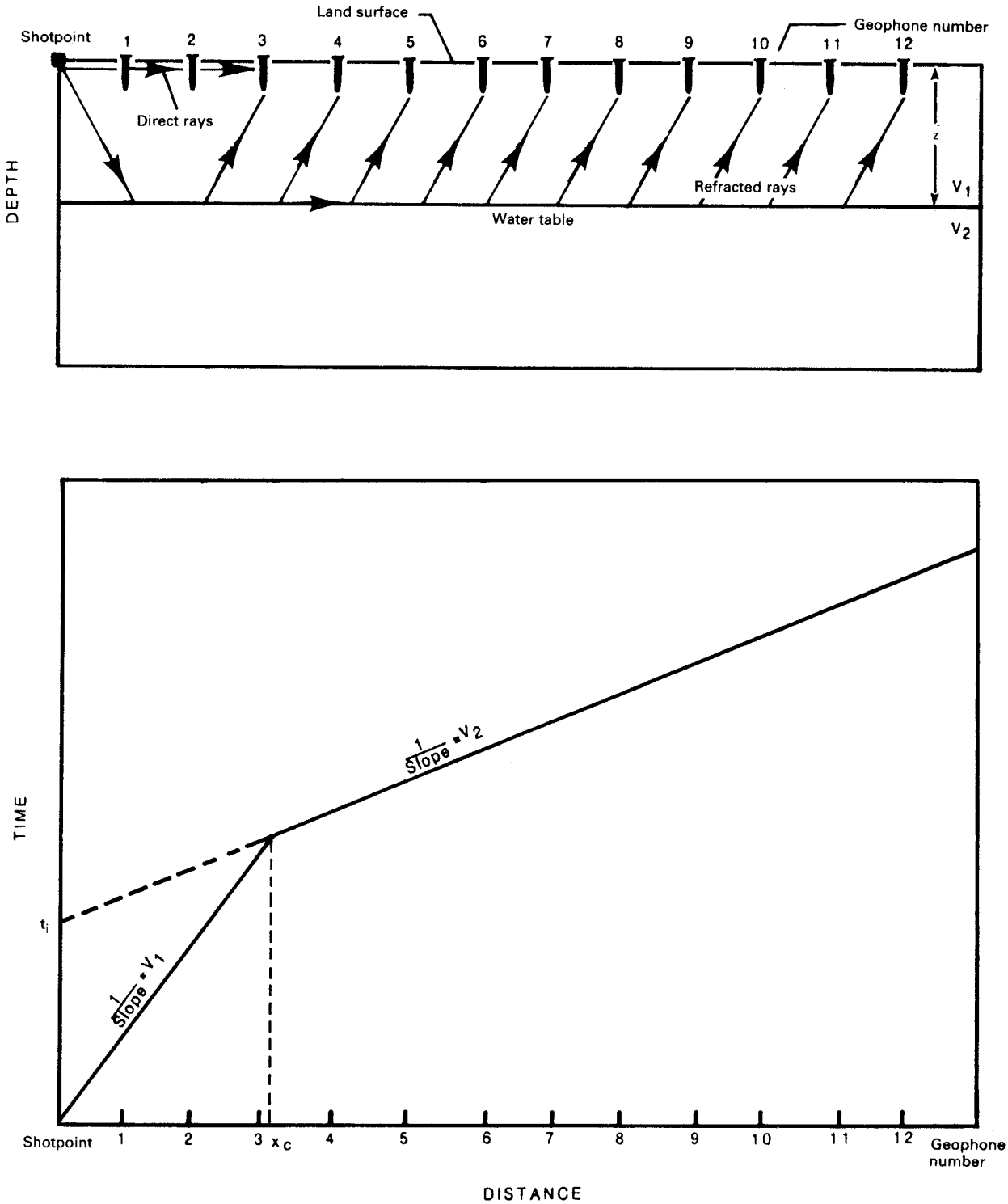

Figure 3.—Seismic raypaths and time-distance plot for a two-layer model with parallel boundaries.

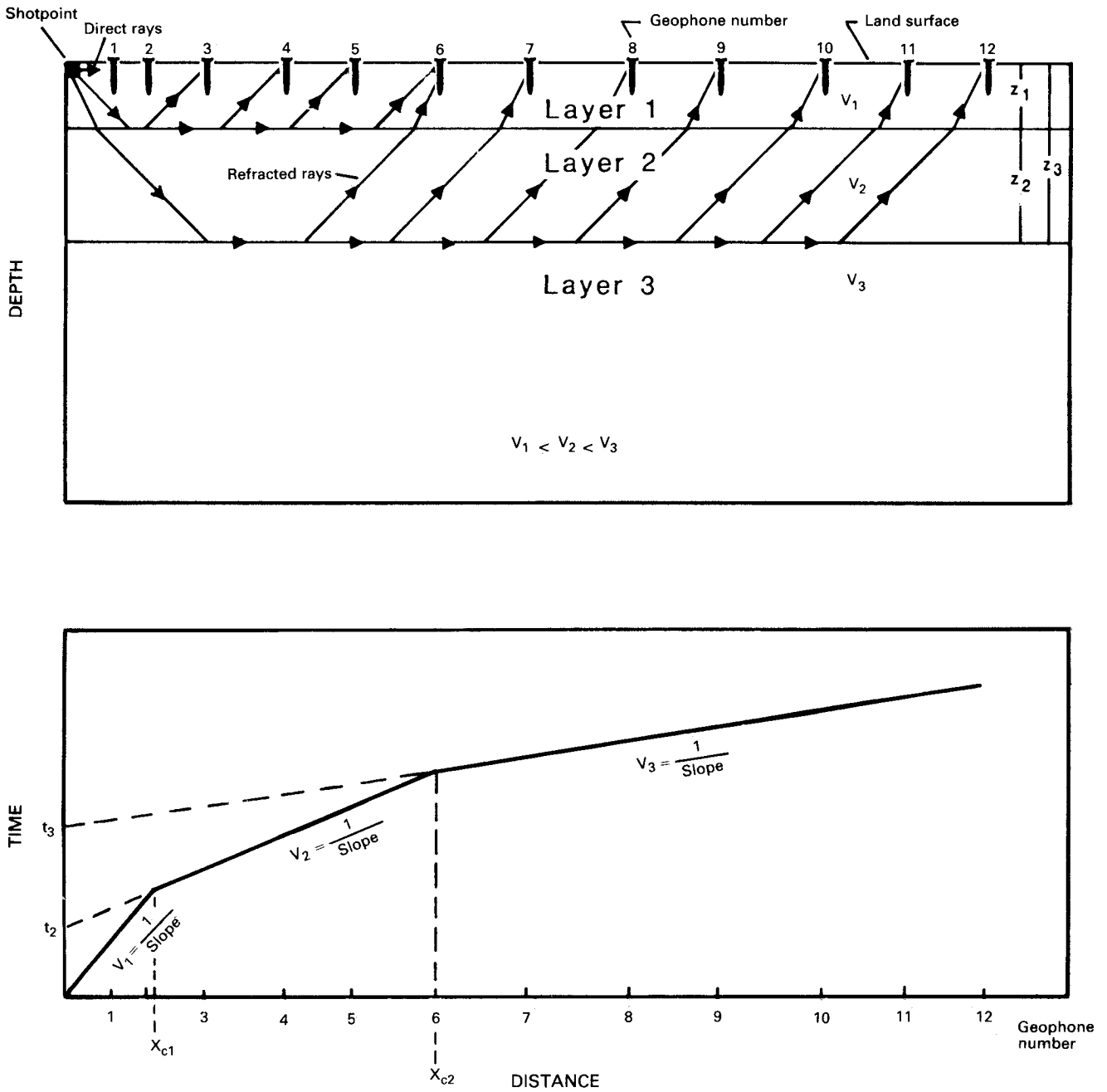

Figure 4.—Seismic raypaths and time-distance plot for a three-layer model with parallel boundaries.

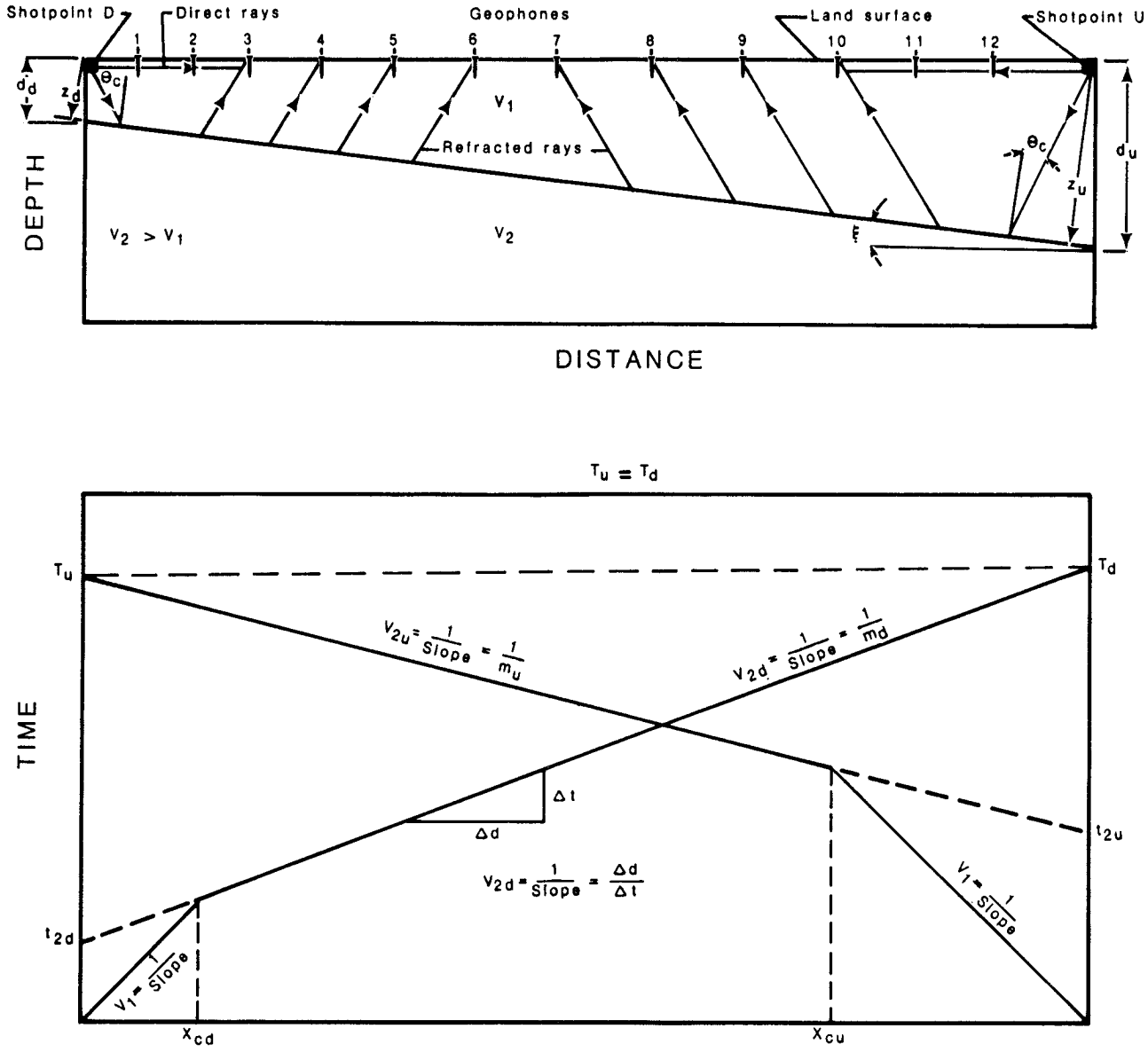

Figure 5.—Seismic raypaths and time-distance plot for a two-layer model with a dipping boundary.

where

θ_c = critical angle,

V_1 = true velocity of sound in layer 1 (from time-distance plot),

m_d = slope of downdip V_2 segment on time-distance plot, and

m_u = slope of updip V_2 segment on time-distance plot.

(b) $$\xi = \tfrac{1}{2}\left(\sin^{-1} V_1 m_d - \sin^{-1} V_1 m_u\right), \qquad (12)$$

where

ξ = dip angle of the refractor.

(c) $$z_u = \frac{V_1 t_{2u}}{2 \cos \theta_c}, \qquad (13)$$

where

z_u = perpendicular distance to refractor at the updip shotpoint (shotpoint 2) and

t_{2u} = intercept time of updip v_2 segment of time-distance plot.

(d) $$z_d = \frac{V_1 t_{2d}}{2 \cos \theta_c}, \qquad (14)$$

where

z_d = perpendicular distance to refractor at downdip shotpoint (shotpoint 1) and

t_{2d} = intercept time of downdip V_2 segment of time-distance plot.

(e) $$d_u = \frac{z_u}{\cos \xi}, \quad (15)$$

where

d_u = extrapolated vertical depth to the refractor beneath shotpoint on updip side (shotpoint 2).

(f) $$d_d = \frac{z_d}{\cos \xi}, \quad (16)$$

where

d_d = extrapolated vertical depth to the refractor beneath shotpoint on downdip side (shotpoint 1).

2. Crossover-distance formulas (Mooney, 1981, p. 10–8):

(a) $$d_u = \frac{x_{cu}}{2 \cos \xi} \frac{V_2 - (V_1 \cos \xi)}{\sqrt{(V_2)^2 - (V_1)^2}} + \frac{x_{cu}}{2} \tan \xi \quad (17)$$

and

(b) $$d_d = \frac{x_{cd}}{2 \cos \xi} \frac{V_2 - (V_1 \cos \xi)}{\sqrt{(V_2)^2 - (V_1)^2}} - \frac{x_{cd}}{2} \tan \xi, \quad (18)$$

where

V_1 and ξ are as defined for equations 11 and 12,

V_2 = true velocity of sound in layer 2 (calculated),

x_{cu} = crossover distance of the updip time-distance segment, and

x_{cd} = crossover distance of the downdip time-distance segment.

Equations 17 and 18 simplify to the following if the dip angle is small and cosine ξ is almost equal to 1.0:

(c) $$d_u = \frac{x_{cu}}{2} \sqrt{\frac{V_2 - V_1}{V_2 + V_1}} + \frac{x_{cu}}{2} \sin \xi \quad (19)$$

and

(d) $$d_d = \frac{x_{cd}}{2} \sqrt{\frac{V_2 - V_1}{V_2 + V_1}} - \frac{x_{cd}}{2} \sin \xi. \quad (20)$$

Example problem

The following example illustrates the use of these formulas and demonstrates the need for choosing the formula most applicable to the field situation.

A. The time-distance plot in figure 6 is obtained in the field by firing only one shot at one end of a seismic-refraction line. If only one shot in one direction is fired, the interpreter would have to use a two-layer horizontal interpretation formula to determine the depth to the refracting layer.

(1) Using the intercept-time formula (eq. 3) to find the depth to the refractor,

$$z = \frac{t_1}{2} \frac{V_2 V_1}{\sqrt{(V_2)^2 - (V_1)^2}}$$

$$= \frac{0.0075}{2} \frac{10{,}600(5{,}000)}{\sqrt{(10{,}600)^2 - (5{,}000)^2}}$$

$$= 21 \text{ ft.}$$

The depth to rock is determined to be 21 ft along the entire profile.

(2) Similar results are obtained using the crossover-distance formula (eq. 6):

$$z = \frac{x_c}{2} \sqrt{\frac{V_2 - V_1}{V_2 + V_1}}$$

$$= \frac{70.4}{2} \sqrt{\frac{10{,}600 - 5{,}000}{10{,}600 + 5{,}000}}$$

$$= 21 \text{ ft.}$$

B. A shot fired from the opposite end of the geophone spread produces a reversed profile. The time-distance plot shown in figure 7 was plotted from the field data.

(1) Using the two-layer, dipping-interface, intercept-time formulas (eqs. 9, 11–16) and the following data obtained from the time-distance plot, the correct depth to the dipping refractor can be calculated.

From the time-distance plot,

t_{2u} = 0.0448 s $\quad$ m_d = 0.0000945

t_{2d} = 0.0075 s $\quad$ $V_{2u} = \frac{1}{m_u}$ = 26,700 ft/s

V_1 = 5,000 ft/s

m_u = 0.0000375 $\quad$ $V_{2d} = \frac{1}{m_d}$ = 10,600 ft/s

(a) $$\xi = \tfrac{1}{2}[\sin^{-1}(V_1 m_d) - \sin^{-1}(V_1 m_u)]$$

$$= \tfrac{1}{2}[\sin^{-1} 5{,}000(0.0000945) - \sin^{-1} 5{,}000(0.0000375)]$$

$$= 8.75°$$

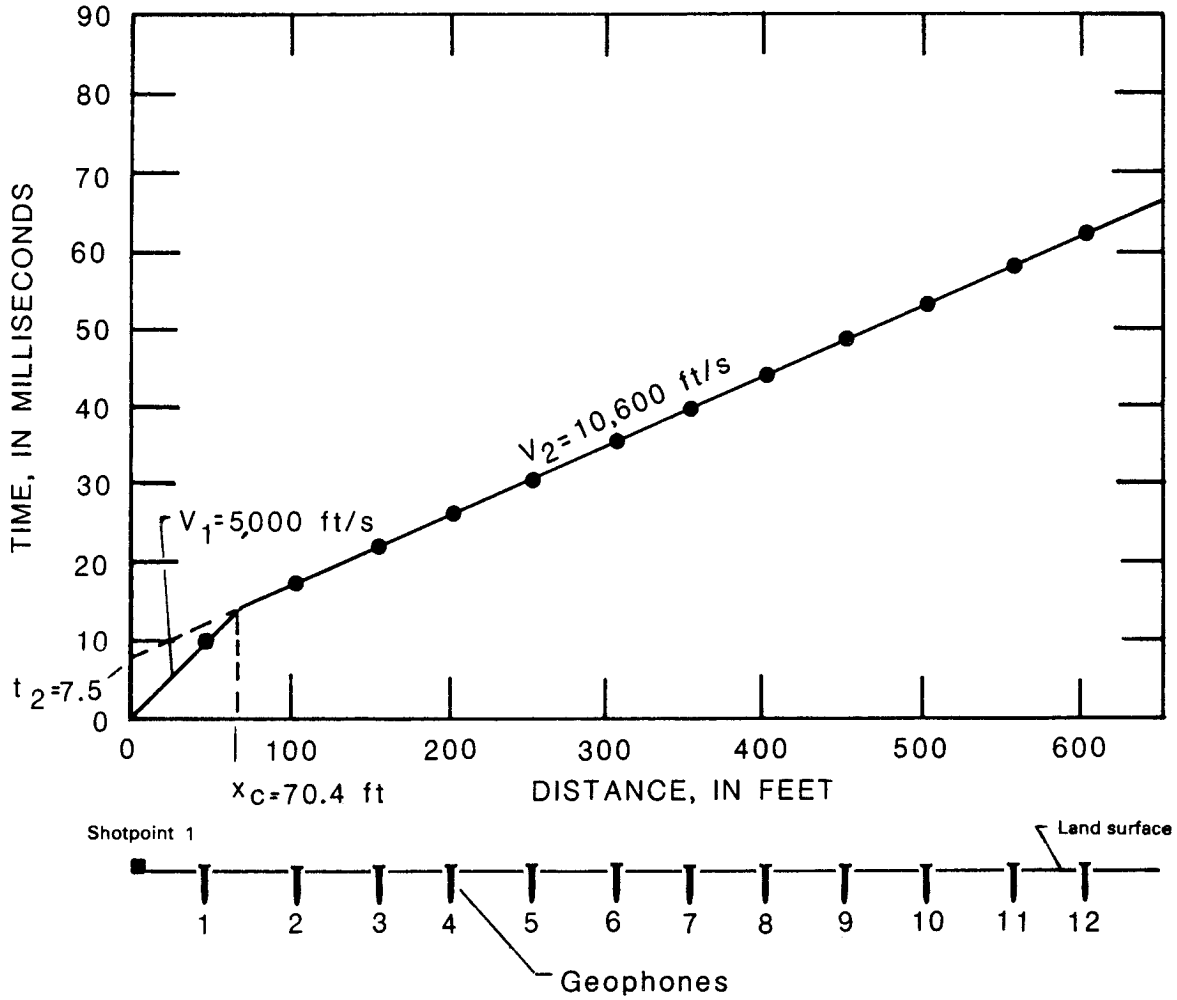

Figure 6.—Time-distance plot resulting from one shotpoint over a two-layer model with a dipping boundary.

(b) $$V_2=\frac{2V_{2u}V_{2d}}{V_{2u}+V_{2d}}\cos\xi$$

$$=\frac{2(26{,}700)(10{,}600)}{26{,}700+10{,}600}\cos 8.75$$

$$=15{,}000 \text{ ft/s}$$

(c) $$\theta=\tfrac{1}{2}[\sin^{-1}(V_1 m_d)+\sin^{-1}(V_1 m_u)]$$
$$=\tfrac{1}{2}[\sin^{-1}5{,}000(0.0000945)$$
$$+\sin^{-1}5{,}000(0.0000375)]$$
$$=19.5°$$

(d) $$z_u=\frac{V_1 t_{2u}}{2\cos\theta}=\frac{5{,}000(0.0448)}{2\cos 19.5}=118.8 \text{ ft}$$

(e) $$z_d=\frac{V_1 t_{2d}}{2\cos\theta}=\frac{5{,}000(0.0075)}{2\cos 19.5}=19.9 \text{ ft}$$

(f) $$d_u=\frac{z_u}{\cos\xi}=\frac{118.8}{\cos 8.7}=120 \text{ ft}$$

(g) $$d_d=\frac{z_d}{\cos\xi}=\frac{19.9}{\cos 8.7}=20 \text{ ft}$$

(2) Using the crossover-distance formulas (eqs. 17, 18) with the same field data, d_u and d_d can again be calculated.

From the time-distance plot,

x_{cd} = 70.4 ft
x_{cu} = 273.8 ft
V_1 = 5,000 ft/s

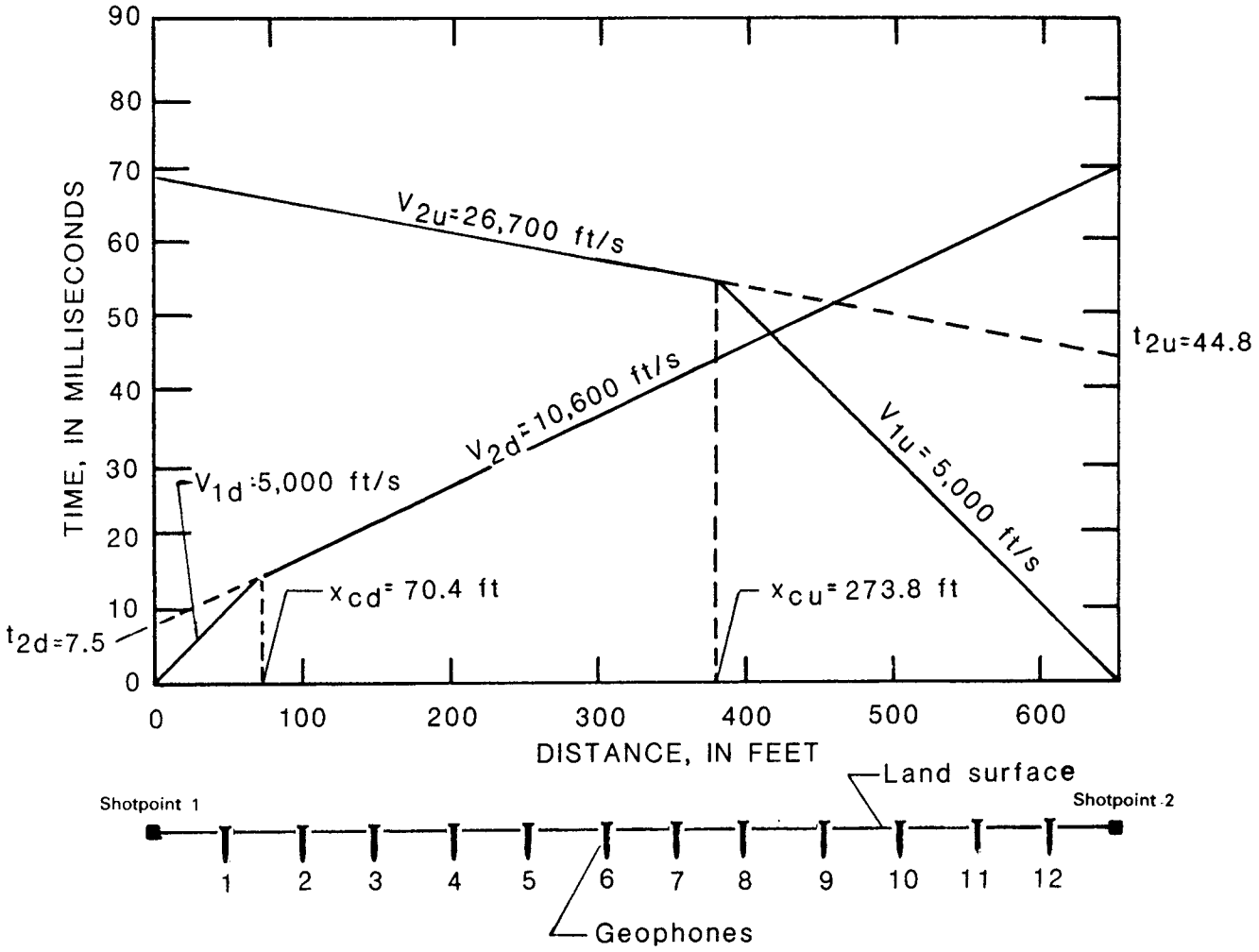

Figure 7.—Time-distance plot resulting from two reversed shots over the two-layer model with a dipping boundary illustrated in figure 5.

(a) $\xi = \frac{1}{2}[\sin^{-1}(V_1 m_d) - \sin^{-1}(V_1 m_u)]$

$= \frac{1}{2}[\sin^{-1} 5{,}000(0.0000945) - \sin^{-1} 5{,}000(0.0000375)]$

$= 8.75°$

(b) $V_2 = \frac{2V_{2u}V_{2d}}{V_{2u}+V_{2d}} \cos \xi$

$= \frac{2(26{,}700)(10{,}600)}{26{,}700+10{,}600} \cos 8.75$

$= 15{,}000$ ft/s

(c) $d_u = \frac{x_{cu}}{2\cos\xi} \cdot \frac{V_2 - (V_1 \cos\xi)}{\sqrt{(V_2)^2-(V_1)^2}} + \frac{x_{cu}\tan\xi}{2}$

$= \frac{273.8}{2\cos 8.75} \cdot \frac{15{,}000-(5{,}000\cos 8.75)}{\sqrt{(15{,}000)^2-(5{,}000)^2}} + \frac{273.8\tan 8.75}{2}$

$= 120$ ft

(d) $d_d = \frac{x_{cd}}{2\cos\xi} \cdot \frac{V_2 - (V_1\cos\xi)}{(V_2)^2-(V_1)^2} - \frac{x_{cd}\tan\xi}{2}$

$= \frac{70.4}{2\cos 8.75} \cdot \frac{15{,}000-(5{,}000\cos 8.75)}{(15{,}000)^2-(5{,}000)^2} - \frac{70.4\tan 8.75}{2}$

$= 20$ ft

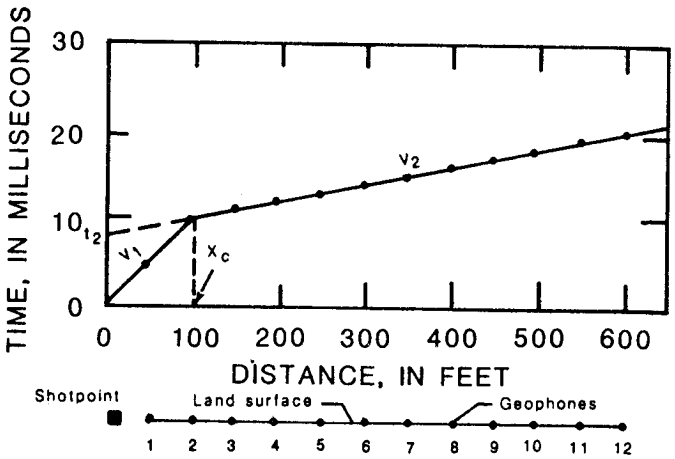

Control for plotting V_2 better than for V_1-- Intercept-time formulas are preferred. V_1 is defined by two points. If the time at geophone 1 was in error, x_c would vary significantly. V_2, however, is defined by many data points and t_2 will not vary with individual arrival time errors.

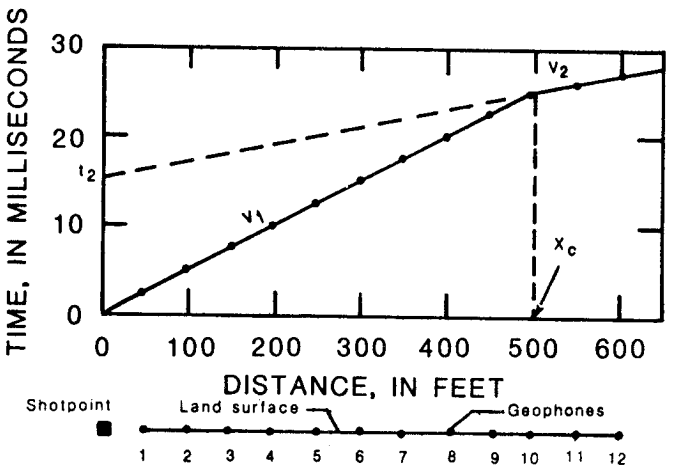

Control for plotting V_1 better than for V_2-- Crossover-distance formulas are preferred. V_2 is defined by three points and an error in the time of geophone 12 would significantly change the intercept time (t_2). The critical distance would not vary significantly.

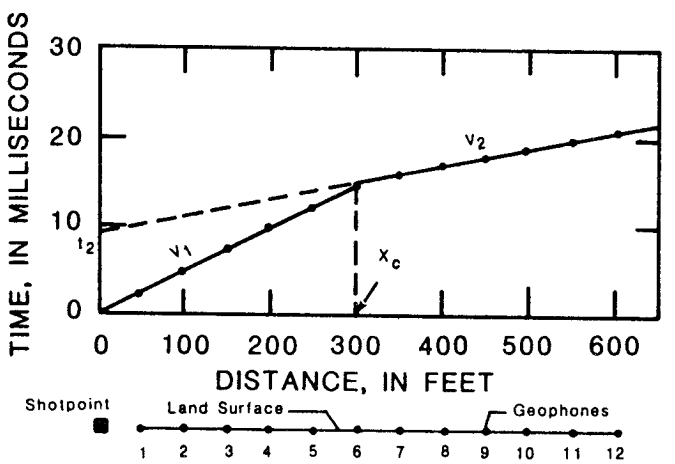

Control for plotting V_1 and V_2 about the same-- Intercept-time and crossover-distance formulas are equal. All line segments are defined by about the same amount of data.

Figure 8.—Advantages and disadvantages of intercept-time versus crossover-distance formulas in determining depth to a refractor under different field conditions.

Summary of example problem:

1. Using a single-shot, nonreversed seismic-refraction profile and the two-layer parallel-boundary formulas, the interpretation gives a subsurface having a velocity of sound in layer 1 of 5,000 ft/s and a second horizontal layer 21 ft deep having a velocity of sound of 10,600 ft/s.

2. Using a reversed seismic-refraction profile and the two-layer dipping-boundary formulas, the correct interpretation gives a subsurface having a velocity of sound in layer 1 of 5,000 ft/s and a second layer dipping at 8.7° and having a velocity of sound of 15,000 ft/s. The depth to this interface is 20 ft at the updip shotpoint and 120 ft at the downdip shotpoint.

Multilayer dipping-boundary formulas

Mota (1954), Johnson (1976), and Knox (1976) have published formulas that apply to problems involving a large number of dipping layers, and nomograms for solving this type of problem have been published by Meridav (1960, 1968) and Habberjam (1966).

In practice, however, it becomes increasingly difficult to distinguish between small, discrete changes in the time-distance plots that actually indicate different layers and small errors attributable to the field process and to nonhomogeneous Earth layers.

Formulas for more complex cases

Other solutions for more complex situations are covered in the literature (Dobrin, 1976), but in general these do not apply to hydrologic problems and consequently are not covered here.

Field corrections

In addition to the theoretical solutions to seismic-refraction problems, corrections for field-related problems have also been developed. The two main types of corrections are elevation corrections and weathering corrections. Both are used to adjust field-derived traveltimes to some selected datum planes, so that straight-line segments on the time-distance plot can be associated with subsurface refractors. These corrections can be applied manually (Dobrin, 1976, p. 335) or by computer (Scott and others, 1972).

Summary

In this section, formulas for both intercept time and crossover distance were presented for determining the depth to a refractor. Several investigators have shown that, in general, the crossover-distance formulas are less prone to error than the intercept-time formulas (Zirbel, 1954; Meridav, 1960) because of the greater difficulty in determining the correct slope of the segments of the time-distance plot compared with determining the crossover distances. Telford and others (1976, p. 279), however, take the opposite view. The final choice of methods, therefore, depends on the quality and quantity of the data on the time-distance plot (Grant and West, 1965, p. 149–150). The time-distance plots shown in figure 8 illustrate the advantages and disadvantages of each method under several different field conditions.

Limitations

Prior to using seismic-refraction techniques, certain problems and limitations need to be considered (Domzalski, 1956; Burke, 1967; Wallace, 1970). Three blind-zone problems that affect the success of using seismic-refraction techniques in hydrologic studies will be discussed further. These are (1) thin, intermediate seismic-velocity refractors, (2) insufficient seismic-velocity contrasts between hydrologic units, and (3) slow-seismic-velocity units underlying high-seismic-velocity units.

Thin, intermediate-seismic-velocity refractor

One of the most serious limitations of seismic-refraction methods is their inability to detect intermediate layers in cases in which the layer has insufficient thickness or seismic-velocity contrast to return first-arrival energy. This problem is critical in water-resources investigations because the intermediate layer may be the zone of interest. For example, saturated unconsolidated aquifer material between unsaturated unconsolidated material and bedrock, or a sandstone aquifer between unconsolidated material and crystalline rock, may not be detected with seismic-refraction methods. These intermediate layers cannot be defined by any alternative location of the geophones or by shallow shotpoints. Deep shotholes may overcome this problem (Soske, 1959), but they are usually impractical under normal field conditions. If the presence of such a layer is suspected, however, calculations can be made to determine its minimum and maximum thickness. Figure 9 shows the wave-front and raypath diagram illustrating a situation in which a 70-ft-thick intermediate-seismic-velocity layer is not detected by first arrivals on the time-distance plot. If the intermediate layer is a thin, intermediate-seismic-velocity layer of till underlying a glacial aquifer, the thickness of the aquifer calculated from the refraction data will be in error (Sander, 1978). Successful interpretation of field data acquired in areas exhibiting this problem is dependent on the correlation of geophysical data with drill holes or knowledge of the local geology.

In the absence of drill-hole data, an unexpected velocity change in the time-distance plot should warn the hydrologist that a thin, intermediate-seismic-velocity layer may be present and that a qualified interpretation is in order. An example of this is shown in figure 10, in which the time-distance plot indicates that a thin, intermediate-seismic-velocity layer may exist, provided the interpreter knows something about the local geology and the speed of sound in the various earth materials near the study area.

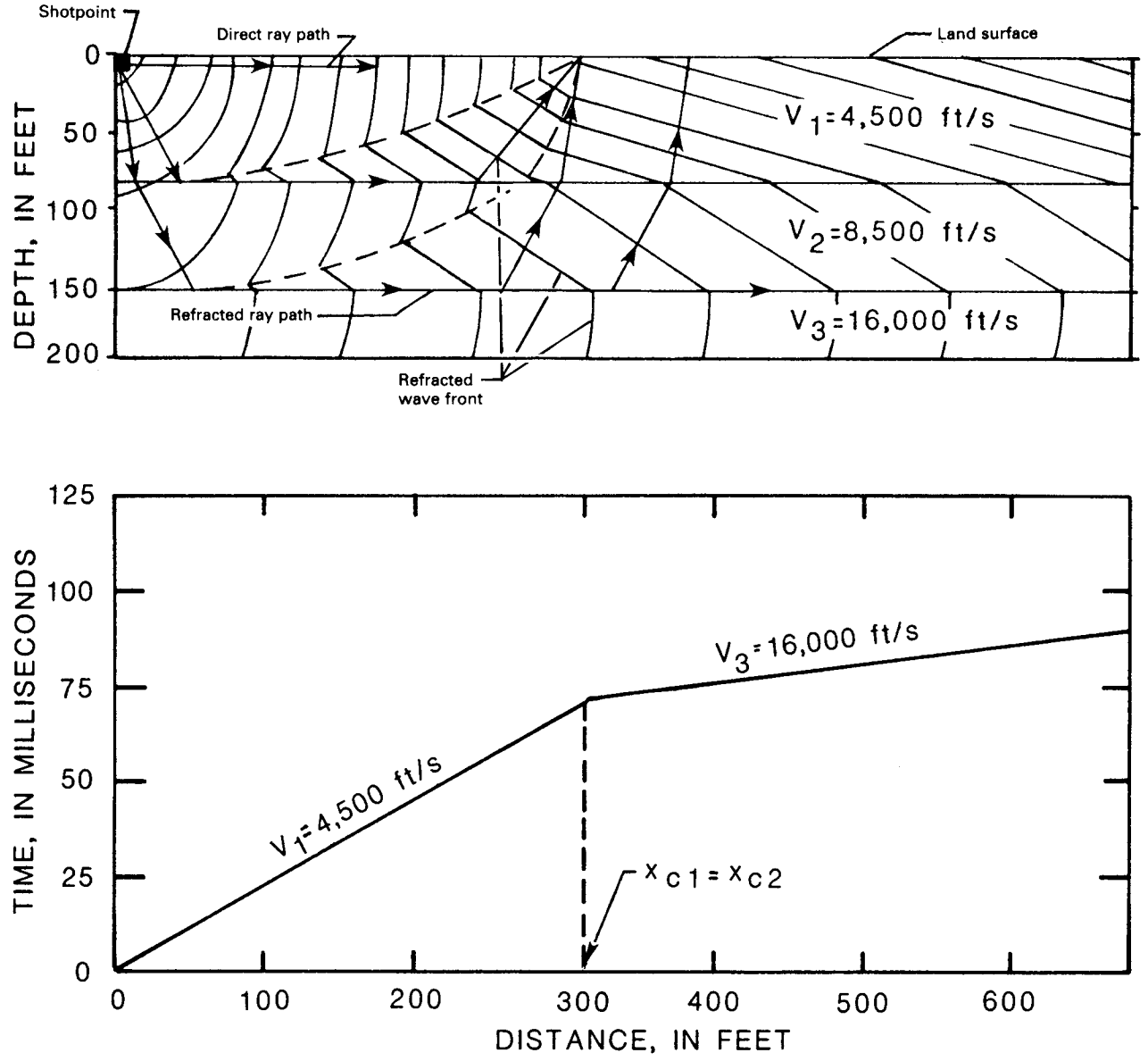

Figure 9.—Seismic wave fronts with selected raypaths and the corresponding time-distance plot for the case of an undetectable intermediate-seismic-velocity layer (modified from Soske, 1959, fig. 4, p. 362).

The case illustrated in figure 10 is very common in hydrologic studies. The unsaturated unconsolidated material has a velocity of 1,000 ft/s, the thin, saturated unconsolidated material has a velocity of about 5,000 to 6,000 ft/s (this layer is not detected by refraction techniques and is not shown in fig. 10), and the crystalline bedrock has a velocity of 15,000 ft/s.

If a thin, intermediate-seismic-velocity layer is suspected, methods are available for determining the maximum thickness of the undetected layer (Soske, 1959; Hawkins and Maggs, 1961; Green, 1962; Redpath, 1973; Mooney, 1981). The following example demonstrates the significance of this problem in water-resources investigations. The calculations in this example and in table 1 are based on a technique described by Mooney (1981, p. 94).

Example problem

The time-distance plot shown in figure 11 is plotted from field data, and the following values are obtained:

x_c = 111 ft (from time-distance plot),
V_1 = 1,500 ft/s (from time-distance plot),
V_3 or V_2 = 15,000 ft/s (from time-distance plot), and
V_2 = 5,000 ft/s (from previous investigations).

A. Assuming that layer 2 does not exist, we would interpret the time-distance plot as a two-layer subsurface (eq. 2):

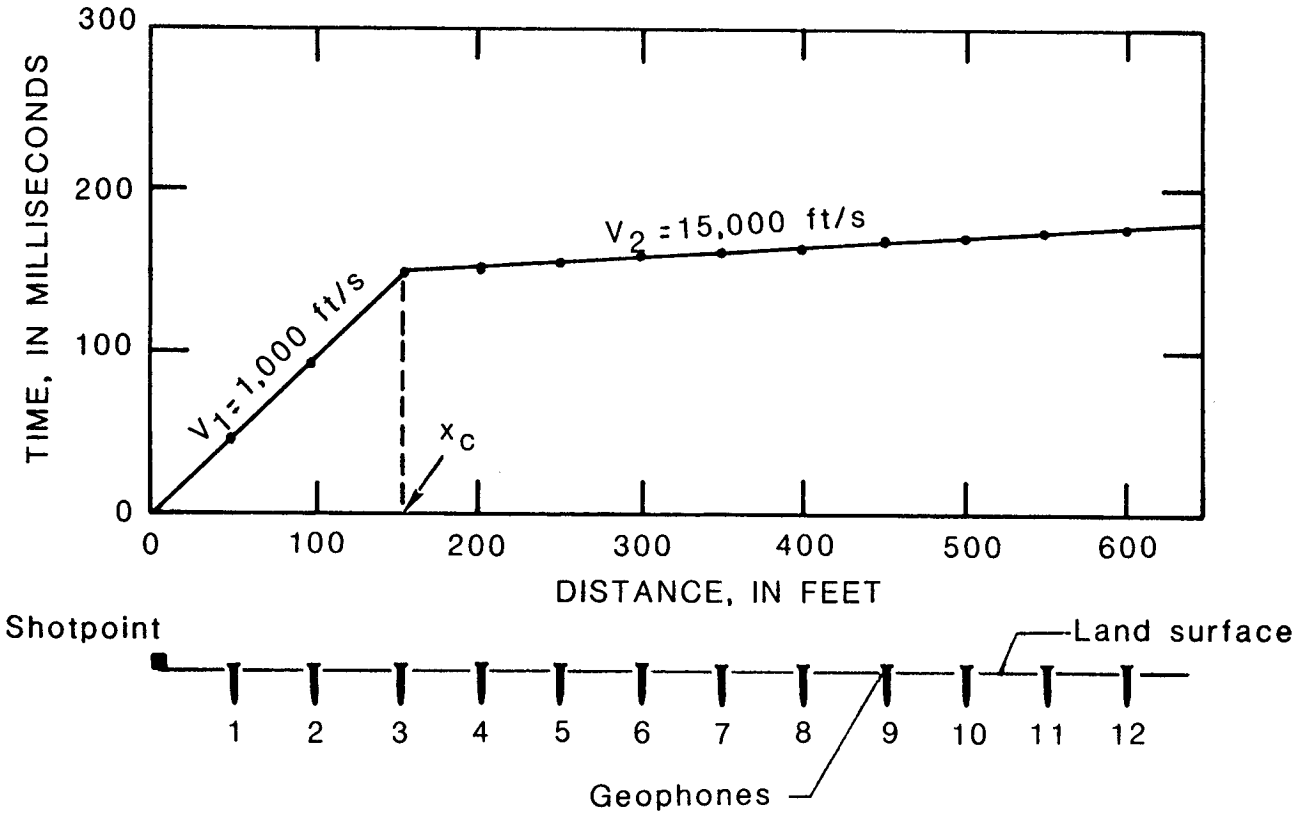

Figure 10.—Time-distance plot showing two layers in an area known to have three layers.

$$\max z_1=\frac{x_c}{2}\sqrt{\frac{V_2-V_1}{V_2+V_1}}=\frac{111}{2}\sqrt{\frac{15{,}000-1{,}500}{15{,}000+1{,}500}}=50 \text{ ft.}$$

The depth to rock using the two-layer interpretation (that is, assuming that there is no saturated material in the geologic section) is, therefore, 50 ft.

B. If the presence of a hidden layer of saturated material is suspected from wells or test holes in the area, the following calculations can be carried out. The minimum depth to layer 2 (the water table) and the maximum possible thickness of undetectable saturated material can be calculated when $x_{c1}=x_{c2}$. (See figs. 9, 11.) In order to calculate these values we assume that a three-layer subsurface exists and proceed with a normal three-layer interpretation using either the time-intercept formulas (eqs. 3–5) or the crossover-distance formulas (eqs. 6–8). A method described by Mooney (1981) using crossover-distance formulas is used in the following calculations.

1. For the depth to layer 2 (the water table),

$$\min z_1=\frac{x_{c1}}{2}\sqrt{\frac{V_2-V_1}{V_2+V_1}}=\frac{111}{2}\sqrt{\frac{5{,}000-1{,}500}{5{,}000+1{,}500}}=41 \text{ ft.}$$

That is, the minimum depth to the water table in the three-layer subsurface is 41 ft.

2. For the depth to layer 3 (the bedrock surface),

$$\max z_3=P(z_1)+\frac{x_{c2}}{2}\sqrt{\frac{V_3-V_2}{V_3+V_2}},$$

where P is defined as

$$P=1-\left(\frac{\frac{V_2}{V_1}\sqrt{\left(\frac{V_3}{V_1}\right)^2-1}-\frac{V_3}{V_1}\sqrt{\frac{V_2^2}{V_1}-1}}{\sqrt{\left(\frac{V_3}{V_1}\right)^2-\left(\frac{V_2}{V_1}\right)^2}}\right)$$

$$P=.86$$

$$\max z_3=.86(40.7)+\frac{111}{2}\sqrt{\frac{15{,}000-5{,}000}{15{,}000+5{,}000}}=74 \text{ ft.}$$

The maximum depth to the bedrock surface is 74 ft.

3. For the maximum undetected thickness of layer 2 (that is, the saturated thickness of the unconsolidated material),

$$\max z_2=z_3-z_1=74-41=33 \text{ ft.}$$

The maximum thickness of an undetected layer 2 in a three-layer subsurface is 33 ft.

In summary, a maximum of 33 ft of saturated sand and gravel under a minimum of 41 ft of unsaturated sand and

Table 1.—*Maximum thickness of an undetectable layer in various hydrogeologic settings*

Hydrogeologic setting and velocity of sound in the geologic units	Thickness of layer 1 (in feet)	Maximum thickness of undetected aquifer material in layer 2 (in feet)	Range in depth to layer 3 (in feet)
Dry sand, V_1 = 1,500 ft/s	10	8	12-18
Saturated sand aquifer, V_2 = 5,000 ft/s	20	16	24-36
	40	33	50-74
Bedrock, V_3 = 15,000 ft/s	50	41	61-91
	100	82	123-182
	200	164	243-364
Till, V_1 = 7,000 ft/s	10	3	11-13
Sedimentary rock aquifer, V_2 = 13,000 ft/s	20	7	22-26
	50	17	55-67
Crystalline rock, V_3 = 15,000 ft/s	100	33	110-133
	200	67	219-267
Saturated sand and gravel, V_1 = 5,000 ft/s	10	6	12-16
	20	12	24-32
Limestone aquifer, V_2 = 10,000 ft/s	50	29	61-79
Crystalline rock, V_3 = 15,000 ft/s	100	58	122-158
	200	115	245-315

gravel could not be detected with the seismic-refraction method in the above example. The depth to rock is between 50 and 74 ft depending on the thickness of the saturated zone. The saturated thickness of undetected sand and gravel is between 0 and 33 ft. The minimum depth to the water table is 41 ft.

Insufficient seismic-velocity contrasts between hydrogeologic units

In many studies, significant hydrogeologic materials may not have detectable seismic-velocity contrasts. Many rock surfaces are not fresh and exhibit different degrees of weathering. As the rock surface weathers, the seismic velocity decreases and is no longer indicative of the unweathered bedrock. In these cases, seismic-refraction techniques may not differentiate the weathered surface from the overlying low-velocity material.

Some significant hydrologic boundaries may have no field-measurable velocity contrast across them and, consequently, cannot be differentiated with these techniques. For example, saturated unconsolidated gravel deposits may have approximately the same seismic velocity as saturated unconsolidated silt and clay deposits (Burwell, 1940).

Low-seismic-velocity units underlying high-seismic-velocity units

In some hydrogeologic settings, the velocity of sound in each of the Earth's layers does not increase with depth, and low-seismic-velocity units underlie high-seismic-velocity units. Examples of this are (1) an unconsolidated sand and gravel aquifer underlying compact glacial tills, (2) semiconsolidated rubble zones beneath dense basalt flows, and (3) dense limestone overlying a poorly cemented sandstone.

In all of these cases, the low-velocity unit will not be detected by seismic-refraction techniques and the calculated depth to the deep refractor will be in error. The reason for this problem is found in Snell's Law, which says that a sound wave will be refracted toward the low-velocity medium. When a low-velocity layer underlies a high-velocity layer, the seismic raypaths are refracted downward or away from the land surface. The sound wave, therefore, would not be detected at the surface until it

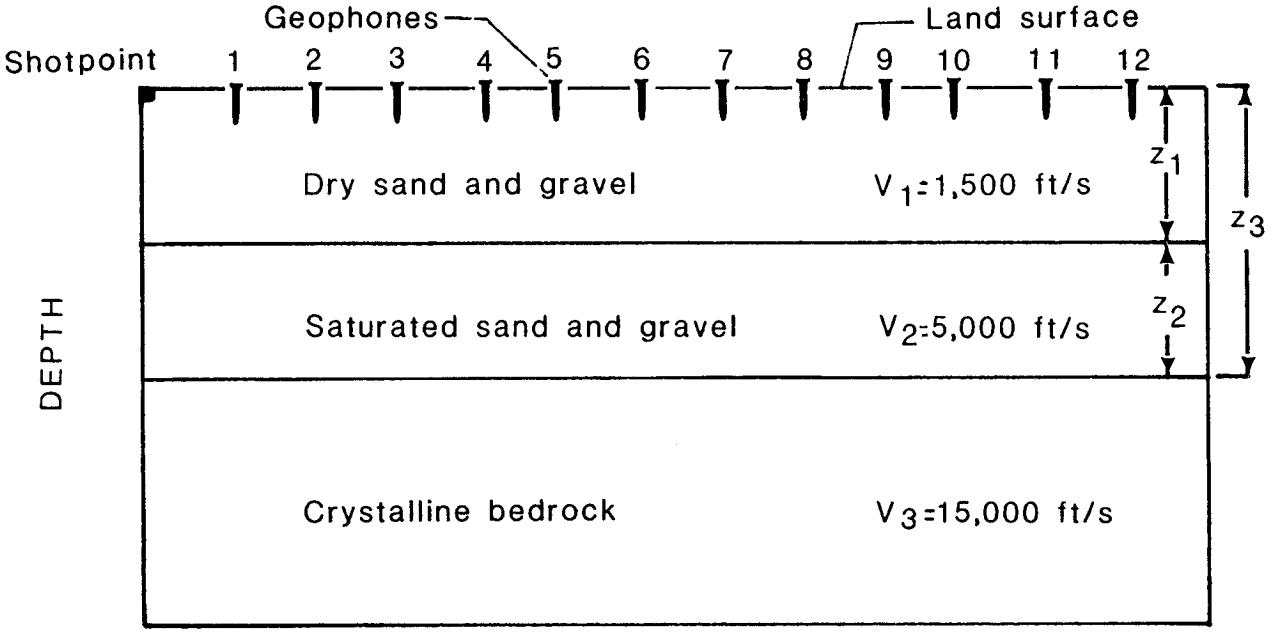

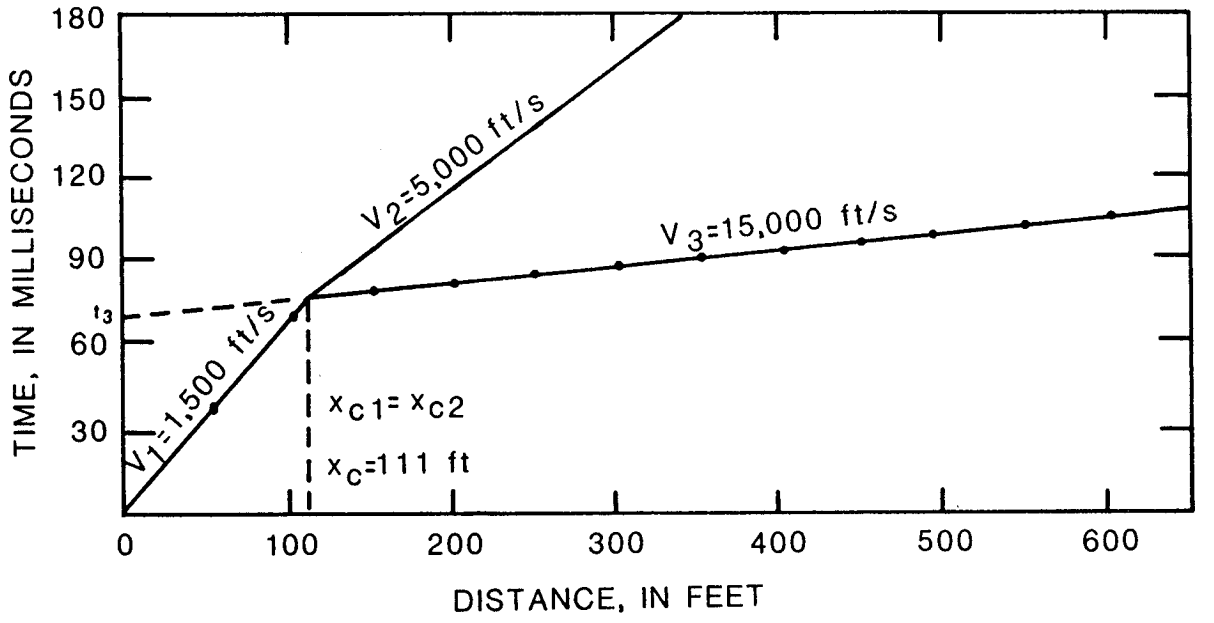

Figure 11.—Seismic section with hidden layer (layer 2) and resulting time-distance plot.

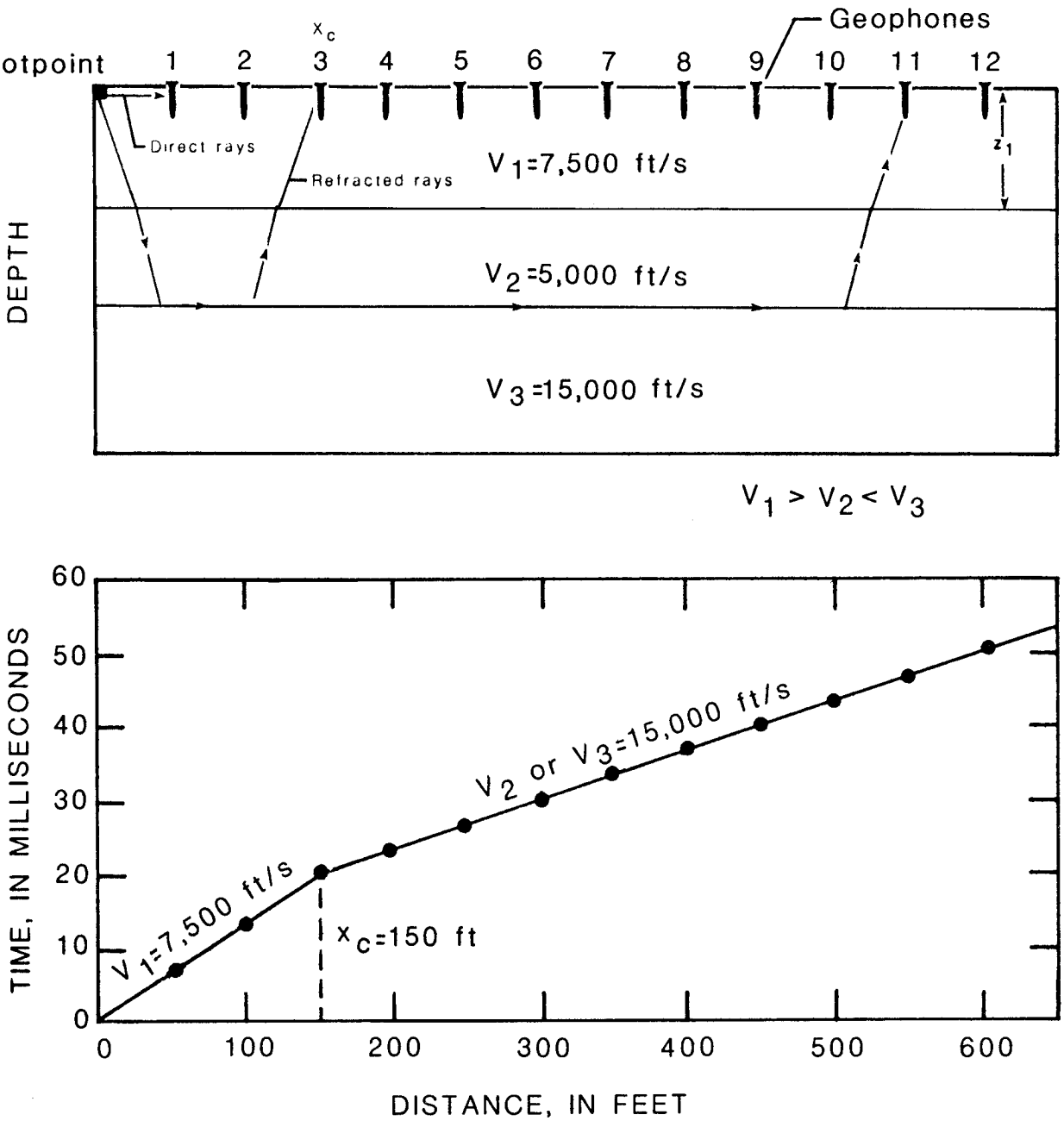

Figure 12.—Seismic section with velocity reversal and resulting time-distance plot.

encountered a layer having a velocity of sound higher than that of any layer previously encountered (fig. 12).

If a low-seismic-velocity unit is known to exist beneath a high-seismic-velocity unit from drill-hole or geologic data, and if its depth and seismic velocity are approximately known, the depth to a deeper refractor can be estimated (Mooney, 1981; Morgan, 1967). Without this information, the depth calculated from the seismic-refraction data will be greater than the actual depth.

Example problem

A. From the field data plotted in the time-distance plot in figure 12, the existence of layer 2 would not be known and an erroneous depth to layer 3 would be calculated if one used the two-layer parallel-boundary formulas (eqs. 3–5):

V_1 = 7,500 ft/s (from time-distance plot),
V_2 = 15,000 ft/s (from time-distance plot),
z_2' = erroneous depth to layer 3, and
x_c = 150 ft (from time-distance plot).

$$z_2' = \frac{x_c}{2}\sqrt{\frac{V_2 - V_1}{V_2 + V_1}} = \frac{150}{2}\sqrt{\frac{15{,}000 - 7{,}500}{15{,}000 + 7{,}500}} = 43 \text{ ft.}$$

The depth to rock using the two-layer interpretation is, therefore, 43 ft. If the thickness and the velocity of sound in layer 2 are known or can be estimated from drill-hole or other data, a more accurate depth can be calculated.

B. From a nearby drill hole and a previous seismic-refraction investigation in a nearby area, it is determined that layer 1 is glacial till approximately 20 ft thick and having a seismic velocity of approximately 7,500 ft/s. It is underlain by saturated sand and gravel having a velocity of about 5,000 ft/s. Now, a more realistic value for the depth to layer 3 (z_2) can be calculated using the following method described by Mooney (1981, p. 9–17):

V_1 = 7,500 ft/s,
V_2 = 5,000 ft/s (from previous investigation),
V_3 = 15,000 ft/s (from time-distance plot),
z_1 = 20 ft (from nearby drill hole), and
z_2 = true depth to layer 3.

$$z_2 = (Q+1)\frac{x_c}{2}\sqrt{\frac{V_3 - V_1}{V_3 + V_1}} - z_1 Q, \qquad (21)$$

where Q is defined as

$$Q = \sqrt{\frac{\left(\frac{V_3}{V_1}\right)^2 - 1}{\left(\frac{V_3}{V_2}\right)^2 - 1}} - 1. \qquad (22)$$

Now substituting,

$$Q = \sqrt{\frac{\left(\frac{15{,}000}{7{,}500}\right)^2 - 1}{\left(\frac{15{,}000}{5{,}000}\right)^2 - 1}} - 1 = -0.39$$

and

$$z_2 = (-0.39+1)\frac{150}{2}\sqrt{\frac{15{,}000 - 7{,}500}{15{,}000 + 7{,}500}} - 20(-0.39)$$

$$= 34 \text{ ft.}$$

In summary, without any external data, a two-layer subsurface with rock at 43 ft was interpreted from the seismic data. Using data from a nearby test hole and the results from a previous seismic-refraction study, a three-layer subsurface with rock at 34 ft was interpreted from the same field data.

One special example of a hidden-layer problem is encountered when seismic-refraction surveys are conducted in areas where the surface of the ground is frozen. The velocity of sound in frozen ground is about 12,000 ft/s (Bush and Schwarz, 1965), and the frozen zone can act as a high-velocity surficial layer. Any layers under the frozen ground cannot be detected unless the velocity of sound in them is greater than 12,000 ft/s. The hydrologist must be careful in interpreting data gathered under these field conditions. Figure 13 shows the time-distance plot that would be obtained in a stratified-drift valley with frozen ground at the surface.

One way to eliminate this problem is to bury both the sound source and the geophones beneath the frozen layer. This usually involves considerable effort and is not economical in most hydrologic programs.

Other limitations of seismic-refraction techniques

The following limitations are mentioned not to discourage the use of seismic-refraction techniques, but rather to make hydrologists aware of potential pitfalls. These situations, recognized early in the study, can be accounted for in the planning, data-acquisition, and interpretation phases of the study.

Ambient noise

Ambient noise, that is, the noise produced by vehicular traffic, construction equipment, railroads, wind, and so forth, has a detrimental effect on the quality of seismic-refraction data. Some solutions to this problem are as follows: (1) decrease the amplifier gains and increase the input signal by using more explosives or repeated hammer blows, (2) reschedule operations for a quiet part of the day, and (3) use selective filters on the seismograph to eliminate unwanted frequencies.

Horizontal variations in the velocity of sound and the thickness of the weathered zone

Horizontal discontinuities in the low-velocity zone near the surface have a significant effect on seismic-refraction studies. This zone usually is the unsaturated zone and typically has velocities of 400 to 1,600 ft/s. Short geographic spreads are needed to determine the velocity of sound and the thickness of this layer. A variation of 1 ft in the thickness of a weathered layer consisting of material having a velocity of sound of 1,000 ft/s causes the refracted sound ray to be delayed or sped up by 1 ms. This same time interval represents 10 ft of material having a velocity of sound of 10,000 ft/s.

Accuracy of seismic-refraction measurements

The accuracy with which the depth to a refractor can be determined by seismic-refraction methods depends on many factors. Some of these factors are

- Type and accuracy of seismic equipment,
- Number and type of corrections made to field data,
- Quality of field procedures,

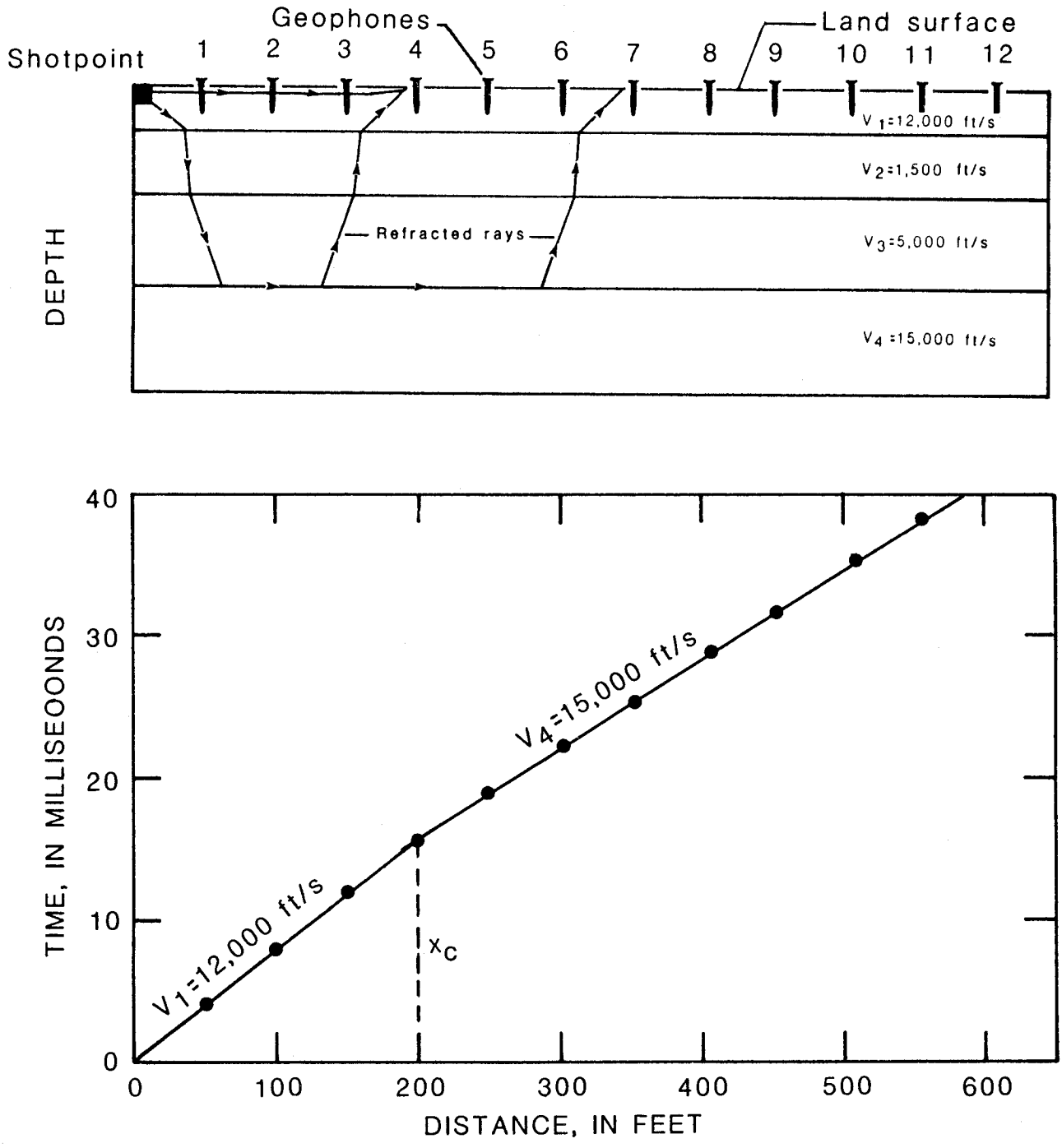

Figure 13.—Interpreted seismic section and time-distance plot for a four-layer model having frozen ground at the surface.

- Type of interpretation method used,
- Variation of the Earth from simplifying assumptions used in the interpretation procedure, and
- Ability and experience of the interpreter.

Published references (Griffiths and King, 1965; Eaton and Watkins, 1967; Wallace, 1970; Zohdy and others, 1974) and the author's unpublished data indicate that the depth to a refractor can reasonably be determined to within 10 percent of the true depth. Larger errors usually are due to improper interpretation of difficult field situations.

Annotated references

Alsop, S.A., 1982, Engineering geophysics: Association of Engineering Geologists Bulletin, v. 19, no. 2, p. 181–186.
[Brief review of the engineering application of seismic-refraction techniques.]